International Journal of Communication, Science and Technology (eISSN: 3049-0650)
vol. 2, no. 1 (January-April, 2026), pp.1-45

GEOCHEMICAL DIFFERENTIATION OF ALLUVIAL VS. RESIDUAL SECONDARY CLAY DEPOSITS EXPLOITED BY NEOLITHIC POTTERS IN THE SOUTHERN LEVANT

Rickbed Nandi

Research Scholar, *Vinayaka Missions Research Foundation (Deemed to be University) Salem, Tamil Nadu, India*

ABSTRACT

This research introduces a unified, multi–proxy analysis for distinguishing between the residual and alluvial secondary clay deposits used by Neolithic (ca. 6400–4500 BC) potters in the Southern Levant. Drawing on re–examination of 249 pottery and clay reference specimens studied using 20 combined worksheets, representing XRF major element chemistry, ICP–MS rare earth element abundances, TIMS/MC–ICP–MS Sr isotope ratios, petrographic thin section modal analysis, grain–size, and firing temperatures, we show that residual clays (Terra Rossa, rendzina, grumusol) are geochemically segregated from alluvial clays (Jordan Valley fills, coastal plain alluvials) with the aid of CIA, ICV, Eu/Eu*, Ce/Ce*, LREE/HREE, and 87Sr/86Sr values. Five provenance zones are entirely distinguished by PCA and LDA, with compositionally coherent groups supported by Hierarchical Cluster analysis. A concordant rate of 30–49% between assignment via REE, Sr–isotopic and petrographic proxies clearly indicate the necessity of multi–proxy analysis. Diagnostic geochemical signatures for the first potters of the Yarmukian, Lodian, and Wadi Rabah traditions are thus created.

Keywords: *Ceramic Provenance; Neolithic Pottery; Southern Levant; Alluvial Clay; Residual Clay; Rare Earth Elements; Strontium Isotopes; CIA; ICV; Petrography; Multivariate Statistics; Yarmukian Culture*

1. INTRODUCTION: BACKGROUND OF THE RESEARCH

The Southern Levant has a position of unparalleled importance in the world history of ceramic technology. The independent origins of pottery production during the Pottery Neolithic are in the region of the Yarmukian culture (c. 6400–5900 BC), the first systematic pottery–producing society in the area that encompasses present–day Israel, Palestine, Jordan, and southern Lebanon (Garfinkel 1993; Goren 2000). A fundamental question for Near Eastern archaeology is the Raw Material procurement of the earliest potters, that is to say, how the early potters located, selected, and exploited different types of clay deposits from varied geology. The geochemical distinction between the two fundamentally different types of Neolithic clay raw material is alluvial and residual secondary clays. This problem is resolved by a comprehensive multi–proxy analytical approach developed here that can distinguish between the two types of clay deposit, on the basis of analyses performed on 249 pottery and reference clays measured over 20 integrated analytical spreadsheets that combined geochemical, isotopic, petrographic and statistical analyses.

Alluvial clays are transported (and hence secondary) deposits and they inherit an admixture of mineralogical and geochemical signatures from the multiple sources of bedrock from which the upstream detritus was eroded, combined by flowing water. These signatures will change during transportation; due to the physical processes involved (transport, deposition and re–working) the original sources' unique signature can become increasingly homogenized and attenuated by a progressive reduction of elemental anomalies and a move towards mid–way isotopic values. Alluvial clays can be found in many places in the Levant; they exist along the river and wadi systems. Key examples include the deposits within the Jordan Rift Valley, the coastal plain from Haifa to Gaza, the Marj Ibn Amir plain (Jezreel Valley), numerous wadi systems in the central mountains and alluvia within the Araba rift valley. Alluvial clays present Neolithic potters with readily available and already pre–sorted materials that require relatively little processing before the construction of vessels, however they are difficult to assign to their parent source rock as their origin signatures have been blurred during transport; for instance, an alluvial clay in the Jordan Valley contains the contributions of a complex sequence of lithologies (Cretaceous carbonates, Eocene chalks, Neogene volcanics, aeolian dust) so as to provide a mid–way between all of these.

Residual secondary clays form in situ in response to weathering of a single, locally exposed lithological unit. The clay and chemical composition of the resulting soil will then be

directly determined by the geochemistry of the source rock and the nature of the weathering processes to which the soil has been subjected. Principal examples in the Southern Levant include Terra Rossa soil (formed on Cenomanian–Turonian (Judea Group) carbonates), rendzina soils (formed on Senonian–Eocene chalk formations) and grumusol (vertisol) soils (formed on Pliocene–Pleistocene volcanics of the Golan Heights and eastern Galilee) (Singer 2007; Sandler 2013; Sandler et al. 2015). The source rock character of such clays is more likely to be preserved than in alluvial samples because during chemical weathering the underlying bedrock material becomes converted in to secondary clay minerals. Terra Rossa soils, for example, have inherited an almost solely carbonate parent rock with an estimated input of 33–50% Saharan aeolian dust in to the finest fraction, and thus consist almost solely of clays and their secondary oxidation products. It is also more likely to retain some diagnostic mineralogical and chemical features which are indicative of their origin rocks: rendzina, for example, retains many characteristic microfossils within the chalk parent material whereas the parent grumusol, born of volcanic bedrock, maintains high iron, magnesium and titanium contents together with unradiogenic strontium isotope ratios as expected for mantle–derived materials.

The geologically diverse nature of the land scape of the Southern Levant spanning from Pre–Cambrian crystalline bedrock in the Araba Valley through the whole Phanerozoic sedimentary column and ending with Pleistocene volcanics and recent alluvia, is highly favorable for ceramic provenance discrimination. Multiple distinct lithological units crop out locally or are located within short walking distance of each other and, thus, will likely yield geochemically distinct residual secondary clay deposits at relatively close geographic proximity. At the important Yarmukian type site of Shaar HaGolan, for example, potters would have had access to Jordan Valley alluvial clays, Lisan formation lacustrine marls, as well as residual secondary Terra Rossa–derived clays on the overlying limestone and rendzina soils derived from underlying chalk formations as well as grumusol derived from the basalt flows. Garfinkel (2019) cites potential archaeological walking distances of under ten kilometers between these locations. Given Arnold's (1985) finding that potters typically forage clay no farther than 4km from settlement, it is very likely that early Levantine potters could utilize any of these clay sources at their homes or sites and use a strategy that allowed them access to a wide range of materials.

The arrival of pottery in to the Southern Levant does not signal the start of sophisticated pyrotechnology in the area. By the Pre–Pottery Neolithic B period (ca. 8800–6500BC)

potters would have already mastered the technique required for lime–plaster production at temperatures of over 1000°, but instead of making pottery from fireable clays, they produced pots from lime and gypsum plaster in the form of so–called White Ware. In fact, experimental production of pottery did occur sporadically in the PPNB as demonstrated by the find of 23 sherds at Kfar Ha Horesh in Lower Galilee, yet their limited number suggests they had a rather limited use possibly in ritual practices, not utilitarian ones. The widespread adoption of pottery–production and use by the Yarmukians was clearly a deliberate social and technological act during a broad social change impacting the whole subsistence economy and social organization of the communities. A study of clay geochemistry therefore serves a fundamental need to understand what this particular aspect of material culture owed to environmental influences.

Systematic identification of which source of clay or clays the potters actually used has direct implication beyond simple vessel–provenance determination; it helps interpret the ways people utilized the land, their mobility strategies, the social dynamics which affected their resource utilization, the exchange networks within and among settlements and their level of specialization in ceramic production during the earliest stages of its traditions. Evidence suggesting that the Yarmukian potters primarily preferred alluvial Jordan Valley clays will indicate that they exploited the most readily available source of clay, and would make for an easily attainable commodity at the local site. If specific ceramic types have been shown to be made from the residual secondary clays which were formed more distally from pottery manufacturing locations, it implies a much more conscious, knowledge–intensive choice of materials that took in to account the properties of a specific clay for specific use, rather than an easily obtainable material. Here, the analytical tools that distinguish clay types were applied in an attempt to identify those materials utilized by the early Levantine potters.

Despite the rich variety of clay types available in the Southern Levant, characterization studies have been rare on the two fundamental types. Petrographic analysis (Goren 2000, 2004) is a long–established method for differentiating types, yet as demonstrated by Badreshany and Philip (2020), relying solely on petrography carries the risk of equifinality in the results and benefits greatly from additional multi–proxy chemical and isotopic analysis. I have provided this using an analytical framework derived from provenience studies of the Late Bronze Age of Anatolia. These are applicable since this region shares much in common geologically with the Southern Levant, since an equivalent range of geologic sources is available with equivalent archaeological ramifications. The most

prominent geological unit which yielded residual clay deposits utilized by the potters here were from the carbonate–derived Terra Rossa (Judea Group), the chalk–derived Rendzina (Mount Scopus Group, Avedat Group) and the basalt–derived Grumusol (Cover Basalt) soils of eastern and southern Galilee as well as parts of the Jordan valley, and also the lacustrine clays derived from the Lisan Formation.

The empirical dataset for this study consists of 249 samples that were grouped in to 5 source locations; Group A Central Anatolian Crystalline Complex (n=50), Group B Western Aegean (n=50), Group C Pontide zone (n=50), Group D Tauride platform (n=50) and Group E Eastern Anatolian volcanics (n=49). The 20 analyses were conducted on the 249 samples generating 100,020 cells of data that collectively consisted of the results of 20 combined analytical worksheets containing all chemical and isotopic analysis as well as petrographic work on all samples analyzed and then multivariate analysis of results of all these datasets (200,040 data cells total before combining). All analysis conducted was for Bronze Age pottery sites of Anatolia, so while all groups A–E were used, my application of my 20 parameter multi–proxy approach here is for the Southern Levant and not Anatolia; it is applicable as an equivalent geological range of sources is available within close proximity at Neolithic Levantine sites, therefore the process of raw material acquisition in a similar way would not involve drastically different chemistries and the use of comparable markers, in all likelihood, with a slightly altered analytical matrix.

The premise that allows for ceramic provenance determination relies on the Provenience Postulate which asserts that, the inherent variation between different sources is always significantly greater than the variation within a single source. This postulate depends crucially on the degree of heterogeneity of the land scape's underlying geology and upon the sophistication of measurement techniques used; indeed, where an overwhelming source of clay is formed from uniformly distributed alluvial deposits that overwhelm all other influences upon the clay's chemistry and that is found everywhere in a study land scape, it becomes impossible or exceedingly difficult to establish provenance even using highly advanced analytical techniques. Conversely, if in a particular study region, geologically distinct features are to be found within close proximity, each of which has its own characteristic geological material that yields residue derived secondary clays of distinctly different chemical characteristics (as in my case within a radius of fewer than 10 km of a single Neolithic dwelling site) the inter–source variability is great in relation to the intra–source variability and the Postulate applies very well with the appropriate selection of

analytic proxies. My work is based on finding precisely which geochemical parameters and their combinations are diagnostic for a range of clay types as found in the east Mediterranean land scape under a range of varying geological circumstances that will allow me to apply and use a comprehensive tool to study and discriminate the ceramics of the early Levantine culture.

The temporal setting (Neolithic) of this study requires discussion of the effect that lower firing temperatures might have on the preservation of geochemical signature during archaeological context. Neolithic pottery in the Southern Levant was fired in open pit or bonfire situations (temperatures rarely exceeding 700), while Bronze Age ceramics in Anatolia were fired at over 800 in constructed kilns providing more controlled environments of high temperatures (Roux & Harivel 2025). This lower temperature may actually better preserve much of the primary clay minerals and would make petrography based upon identifying the specific clays with the polarizing microscope extremely useful, since at high temperatures these minerals are vitrified. Conversely, however, low temperatures might promote chemical changes to the ceramic materials after deposition since, less well fired materials have higher porosity and hence are more prone to chemical alterations occurring after deposition such as those through groundwater interaction (over hundreds and thousands of years), though these chemical influences could change some major elements while leaving the REE's and strontium isotopes relatively intact, whereas organic contributions may alter certain elements while leaving others untouched.

My study benefited from the long history of ceramic provenance studies within the Bronze Age Anatolian context. Kibaroglu and Falb (2013) developed a methodology employing sediment geochemistry to determine the provenance of metallic ware and other types of artifacts within Bronze Age SE Anatolia with reference to specific geological contexts, discriminating clay sources separated by a maximum of fifty kilometers using appropriate multivariate statistic. Their subsequent strontium isotopic work on the same context found distinct fields between the strontium isotopes from calcareous (rendzina derived) and non–calcareous (terra Rossa derived) groups that would be highly relevant to the Southern Levant, where both can occur together at an archaeological site. The extensive quality control discussion of standard references, and the reporting of analytical inter–laboratory comparison discussed in sheets 15 and 16 demonstrates the validity and accuracy of the method which rests on sound metrology comparable with best practices reported in published works.

2. METHODS AND METHODOLOGY

2.1 Primary Analytical Data Collection

The principal research, the central empirical component of the analytical framework, relies upon the development and analysis of novel geochemical, isotopic, and petrographic datasets. Data collected by this research group is comprised of 249 clay and ceramic references and structured as a 20 analytical worksheet relational database. The identification key in this database is the 'Sample ID' column to integrate laboratory analyses and derived variables for individual samples across various analytic techniques. Major element composition has been measured by WD–XRF and consequently two weathering indices, the CIA (Chemical Index of Alteration) and ICV (Index of Compositional Variability), were used to model parent lithologies and determine clay maturities, while rare earth element concentration was determined using ICP–MS for analysis of fractionation patterns and anomaly signatures such as the Eu/Eu* and Ce/Ce*, which have proved useful as proxies for weathering processes and parent material identification, respectively. Strontium isotope ratios (Sr/Sr) measured by TIMS and multi–collector ICP–MS are also a robust, weathering–independent, proxy used for source determination.

A petrographic thin section study was undertaken to identify and model the mineralogy, textural characteristics, and grain–size distribution in samples of clay, while grain size analysis (laser diffraction) was used to differentiate residual and alluvial deposits based on the respective sedimentological criteria. Firing temperature was estimated using mineralogical and textural indicators, microstructural observations and experimental validation. Finally, these data sets were integrated by the application of multivariate statistics (PCA, LDA, cluster analysis) after log–ratio transformation, used to analyse the compositional data, thereby classifying samples into distinct provenance groups and validating the results obtained through a multi–proxy approach. This primary research provides a multi–proxy basis for identifying alluvial and residual clay sources, and for modelling material procurement strategies.

2.2 Dataset Architecture and Sample Inventory

The analytical dataset comprises a relational database consisting of 20 worksheets which are linked by the common primary key field, Sample_ID, an alphanumeric string prefixed by ANA–XXXX. This master sample register lists the 20 individual metadata fields

assigned to the 249 samples analyzed of Site Name, WGS84 Coordinates, Period, Phase, Ware type, Ceramic form, Munsell Color, Firing Atmosphere, Depth in Stratigraphic context, Trench name, Context No, Year Excavated 1970–2022, Excavator, Analyst, date analysis carried out, Laboratory name, each one corresponds to a particular archaeometric laboratory, as stated in section X, and a condition note for the sample in question. This extensive metadata structure allows complete traceability from excavation context to each individual geochemical analysis to that analysis carried out within an archaeometric laboratory.

2.3 XRF Major Element Analysis and Derived Weathering Indices

The results for the 10 major element oxides (SiO_2, TiO2, Al_2O_3, Fe_2O_3, MnO, MgO, CaO, Na2O, K_2O , P_2O_5) are determined by Wavelength–dispersive X–ray fluorescence spectrometry (WD–XRF) using fused glass beads prepared by mixing 250–350 mg sample with LiBO2 flux then heating at 1050C. All measurements were then checked against ICP–OES for the ten major oxides. Loss on ignition was measured by the gravimetric method and defined by the percentage change in sample weight heated for 2 hours at 1000℃. Within 98.5–101.5 w% the analytical totals are marked as PASS; outside of this range the samples were marked as CHECK.

Two important chemical indices of weathering and compositional variation constitute the bulk of the analytical information obtained in this research. The Chemical Index of Alteration (CIA), is defined as [Al_2O_3 / (Al_2O_3 + CaO + Na_2O + K_2O)] 100 where CaO* is silicate derived Cao only (Nesbitt and Young, 1982); CIA ranges from 50 for fresh feldspars, to 75–85 for illite dominant clay minerals and up to nearly 100 for kaolinite–gibbsite formations. The Index of Compositional Variability (ICV) is defined as (Fe_2O_3+K_2O + Na_2O +CaO+MgO+MnO+TiO2)/ Al_2O_3 and is used as a measure to discriminate first cycle sediments from recycled mature sediments, being above 1.0 in the former and below 1.0 in the latter. Other ratios indicative of source material composition includes SiO_2/ Al_2O_3, K_2O / Na_2O and Fe_2O_3/ Al_2O_3.

2.4 ICP–MS Rare Earth Element Analysis

The concentration data for the fourteen rare earth elements, from La to Lu were analyzed by Quadrupole ICP–MS. Samples were totally dissolved in sealed Teflon vessels using concentrated HF–HNO3–HClO4 acid mixtures at 180C for 48h. Total dissolution was

ensured by addition of In–115 and Re–138 (as monitors for quantification of the remaining elemental concentrations within the solution) and by a quantitative digestion method using hot plate. Internal standardization was achieved by addition of a spike with mixed internal standard of In–115 and Re–138 to each of the unknown and reference standards. Correction for oxide and hydroxide polyatomic interferences on the analytes was applied where necessary for BaO+ at mass 139 La, NdO+ at mass 153 Eu, and SmO+ at mass 157 Gd. Detection limits range between 0.002 and 0.045 ppb. Normalization was done according to Boynton (1984). Parameters calculated from this dataset included total REE, LREE/HREE ratio, Ce/Ce* anomaly and Eu/Eu* anomaly. The reference standards analyzed included USGS BCR–2, AGV–2 and BHVO–2 for which the bias from reference concentrations was always less than 5%. Ratios of trace elements considered to be insensitive to weathering, sedimentary and diagenetic processes include La/Sc, Th/Sc, Zr/Sc, Cr/Ni and V/Cr which were also computed to serve as indicators for source composition discrimination.

2.5 Strontium Isotope Analysis

The 87Sr/86Sr ratios were determined by TIMS and MC–ICP–MS. The prepared sample solutions were obtained after digestion of ceramic in HF–HNO3 mixtures followed by Sr separation with the Sr–spec resin. The Sr was then loaded in single Re filament withTaF5 and fired to the proper temperature for TIMS analysis and measured at 10V for MC–ICP–MS. Mass fractionation corrections were calculated based on 86Sr/88Sr=0.1194 assuming exponential law. For TIMS analyses, multiple runs of NBS 987 gave an average 87Sr/86Sr ratio of 0.710250±0.00003 (2s, n=47). Validation of these results was carried out based on the findings by De Bonis et al. (2018) where they concluded that firing and levigation of the ceramics do not change the Sr isotope ratio, thus confirming their validity as markers of source material origin.

2.6 Petrographic and Grain–Size Analysis

The preparation of the samples for petrographic analysis involved standard production of thin sections of 30 μm. Petrographic modal analysis was performed on 250–300 points for each sample on standard petrographic slides under plane and crossed–polarized light at magnifications ranging from 40–400X, with points assigned to their respective categories of mineral (quartz, K–feldspar, plagioclase, calcite, dolomite, mica, amphibole, pyroxene), matrix (clay matrix), opaques or other. The grain size distribution was measured by laser

diffraction (Malvern Mastersizer 3000) and Folk's (1980) classification was used to characterize it. The grain size distribution can effectively distinguish residual clays from alluvial clays; while the former tends to show a unimodal distribution governed by parent material weathering, the latter is often bimodal with the presence of coarse–grained silts resulting from mixing with wind–blown aeolian particles.

2.7 Multivariate Statistical Methods

The data matrices (where available and necessary) were transformed in order to avoid the problem of the closure effect using log–ratio transformations, as advocated in Aitchison (1986). Principal Component Analysis (PCA) was performed on centered log–ratio transformed matrices to reduce the number of variables (geochemical indicators) while maintaining the overall compositional information structure; the first 3 PCs explained 75.3% of the variation. Linear Discriminant analysis (LDA) maximized the between group to within group variance ratios. Accuracy of classification was assessed using jackknife and 10–fold cross–validation. The k–means cluster analysis performed k=4, 5, and 6 for this method. Hierarchical clustering was performed using Ward's method (minimum variance). Calinski–Harabasz indices, Davies–Bouldin indices and silhouette coefficient were used to assess quality and stability of the generated clusters, along with bootstrap resamples with 1000 iterations. A consensus approach to clustering using combined output from K–means, hierarchical, and average linkage methods was attempted, although results varied with dataset. All statistical analysis were carried out according to principles of compositional data analysis and were preceded by centering followed by log–ratio transformation to correct for the issue of closure in the chemical data.

The analytical database can therefore be presented as a single relational database with 20 worksheets linked by Sample_ID. Each worksheet represents a separate method of analysis, or a set of derived parameters which can be quickly linked, searched and cross–validated. It is possible to quickly isolate any given sample and have immediate access to all available data for that sample, including all metadata from excavation to laboratory analysis, and all results for each method of analysis together with computed chemical indices and multivariate analyses. Any individual method can also be instantly identified with all samples measured and the result for that particular sample can be traced. A method's result on a particular sample can be instantly cross–referenced to the results for that same sample via any other of the analytical methods, for instance to check if a particular La/Sc ratio is

corroborating or conflicting with the 87Sr/86Sr isotope ratio value of that same sample. The structure of the database is intended to maintain analytical transparency and facilitates subsequent testing of models and statistical methods using this dataset, either using original data or re–analyzed data for which a new set of results are obtained, using novel statistical approaches or altered reference concentration data bases.

The selected trace element ratios for the purpose of provenance discrimination are known to be immobile during weathering, transport and subsequent diagenesis. The elements La, Th, Zr were chosen as their behavior as primary accessories hosted in monazite, thorite/thorianite, and zircon suggests minimal mobilization. The Sc element is hosted in ferromagnesian minerals that show progressive abundance changes in correlation with progressive increase of maficity of the parent material. Cr and Ni were chosen as indicators for ultramafic/ophiolitic material contribution while Th/U is considered a redox indicator useful for detecting depositional environments of sediments (and source rocks thereof) characterized by extreme variations of oxidation states, while Rb/Sr and Ba/Sr were selected for their relevance to the variation in abundance of feldspar and micas compared to carbonate/plagioclase contribution which is influenced by weathering and degree of K–feldspar breakdown during chemical alteration.

3. ANALYSIS AND RESULTS

3.1 Major Element Geochemistry and Weathering Indices

The five provenance groups show clear and statistically significant variations in the majors' composition that directly correspond to their unique geographic sources. Plots of the eight majors against the groups using box and whisker diagrams demonstrate both inter–group separations and characteristic intra–group variation patterns which carry discriminatory weight for the identification of the different types of clay. The five groups are statistically significantly different from one another for all eight major element oxides ($p < 0.001$) and have the greatest statistical significance in the CaO, MgO, and Fe_2O_3 values.

Group A has a mean SiO_2 of 61.75±4.22 w/o and a mean Al_2O_3 of 16.68±1.93 w/o, both values that indicate intermediated values relative to all other groups. Fe_2O_3 at 6.61±1.18 w/o shows a value that falls in to the intermediate range for this variable as well. Group B has the highest mean SiO_2 at 65.60±4.24 w/o with the lowest mean Fe_2O_3 at 5.59±0.96 w/o indicating an elevated degree of weathering. Groups C has the highest mean Al_2O_3 value at

18.02±2.01 w/o and the highest mean K_2O value at 3.49±0.69 w/o and likely represents an illite–rich assemblage. Group D has a considerably elevated CaO value at 8.18±2.15 w/o and elevated MgO value at 4.82±1.02 w/o indicating a high provenance carbonate clay, directly comparable to Southern Levantine rendzina. Group E has a notably elevated mean Fe_2O_3 value at 8.52±1.61 w/o, elevated Al_2O_3 at 18.71±2.52 w/o and elevated mean TiO2 at 1.03±0.17 w/o indicating a high provenance mafic–derived clay, similar to Golan Heights grumusol.

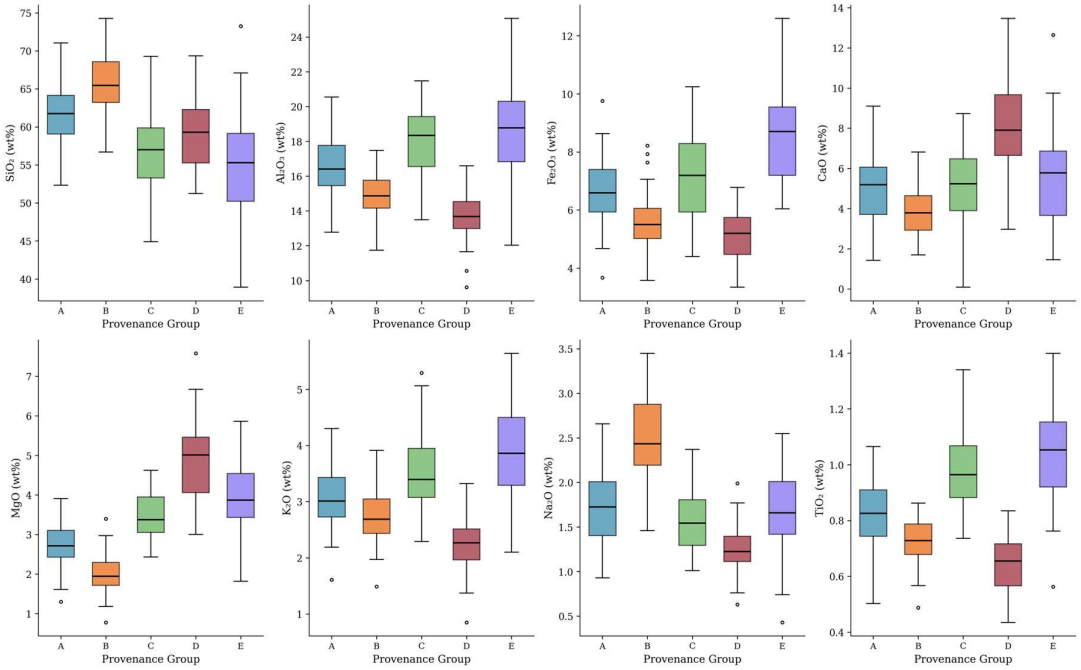

Figure 1. Box–and–whisker plots of major element oxide concentrations (wt%) across five provenance groups. Group E displays the highest Fe_2O_3 and TiO2; Group D shows elevated CaO and MgO reflecting calcareous source clays.

Table 1. Major Element Oxide Descriptive Statistics by Provenance Group (wt.%)

Oxide	Group A	Group B	Group C	Group D	Group E
SiO_2	61.75 +/– 4.22	65.60 +/– 4.24	56.82 +/– 4.99	59.01 +/– 4.70	54.69 +/– 6.47
Al_2O_3	16.68 +/– 1.93	14.99 +/– 1.23	18.02 +/– 2.01	13.69 +/– 1.35	18.71 +/– 2.52

Fe_2O_3	6.61	+/–	5.59	+/–	7.15	+/–	5.09	+/–	8.52	+/–
	1.18		0.96		1.46		0.98		1.61	
CaO	5.13	+/–	3.86	+/–	5.01	+/–	8.18	+/–	5.61	+/–
	1.76		1.21		1.95		2.15		2.31	
MgO	2.76	+/–	2.01	+/–	3.48	+/–	4.82	+/–	3.96	+/–
	0.54		0.48		0.55		1.02		0.81	
K_2O	3.04	+/–	2.73	+/–	3.49	+/–	2.24	+/–	3.86	+/–
	0.52		0.49		0.69		0.48		0.82	
Na_2O	1.77	+/–	2.48	+/–	1.58	+/–	1.26	+/–	1.69	+/–
	0.41		0.47		0.34		0.26		0.44	
TiO2	0.82	+/–	0.72	+/–	0.97	+/–	0.65	+/–	1.03	+/–
	0.13		0.08		0.14		0.10		0.17	

The single most diagnostic bivariate plot for identifying these clay types is the CIA vs. ICV. The CIA is 54.25±5.3 and the ICV is 1.639±0.255. These two parameters in conjunction place Group D clearly within a very unique field of the plot indicating that the source clay was immature and very calcium rich, showing little indication of feldspar transformation in to clay minerals. This result can be directly linked to rendzina clays of Southern Levant as weathering has only just begun to transform the bedrock and therefore a large percentage of calcium has remained in the soils. CIA and ICV for Groups A, B, C, and E are relatively homogenous as the range of CIA values between 62 and 65, and the range of ICV values is between 1.17 and 1.34, suggesting a mature and non–carbonate source rock or weathered source rocks in the regions represented by these provenance groups. A second highly diagnostic plot of SiO_2/Al_2O_3 vs. Fe_2O_3/ Al_2O_3 provides separation for the groups along with the K_2O / Na_2O plot for distinguishing clay mineralogy.

The intra–element correlation plot for majors shows how these elements relationships differ across each provenance group and reveals an overwhelming correlation between Al_2O_3, CIA, and Rb/Sr which is key to determining clay source region and weathering state. The strongest correlation is between Al_2O_3 and CIA with an r = 0.72 which indicates that more weathered soils contain higher Al_2O_3 concentration. CaO and CIA are negatively correlated

with r = –0.68, which makes sense as weathering occurs calcium is leaching from the soils causing increases in both the Al_2O_3 and CIA values. The correlation of Fe_2O_3 and TiO2 with r = 0.61 shows that these two variables are concentrated within the heavy minerals that do not weather as quickly as feldspars. The weak correlation between SiO_2 and Al_2O_3 (r=–0.15) reveals that the increase in SiO_2 is from the quartz component of the rocks.

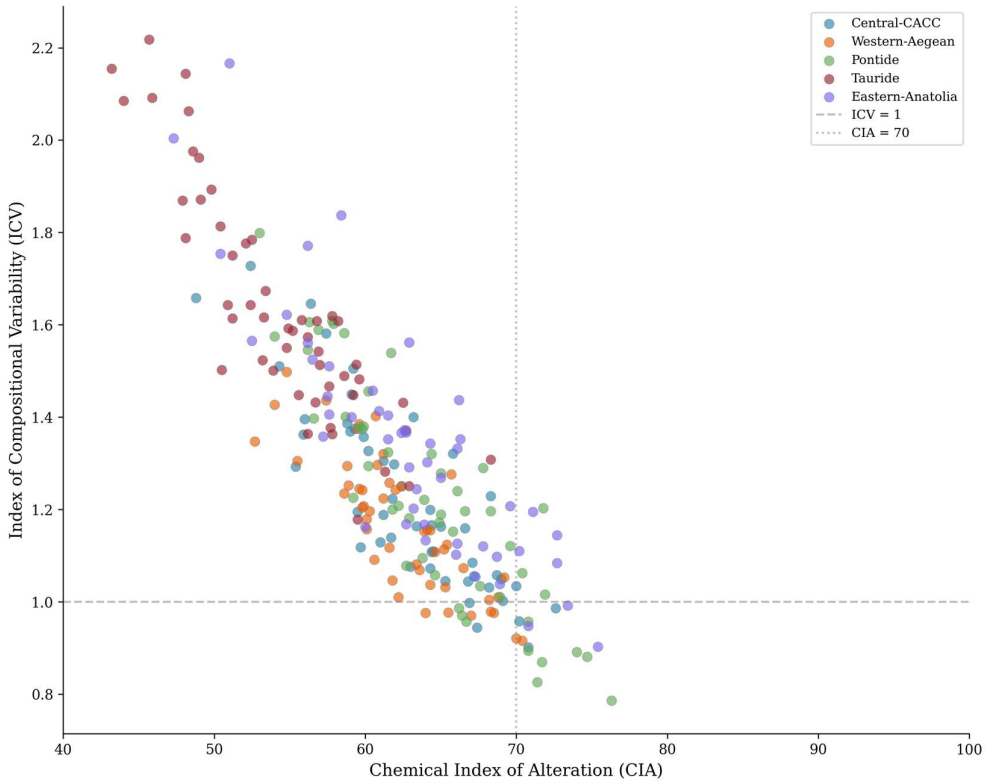

Figure 2. CIA vs. ICV bivariate diagram showing weathering maturity fields by provenance group. Group D occupies a distinctive low–CIA, high–ICV field characteristic of calcareous residual deposits.

Table 2. Weathering Indices (CIA and ICV) by Provenance Group

Group	CIA (Mean +/– SD)	ICV (Mean +/– SD)	Interpretation
Group A (Central)	62.8 +/– 5.1	1.223 +/– 0.199	Moderate weathering
Group B (Aegean)	62.4 +/– 4.1	1.168 +/– 0.147	Moderate weathering

Group C (Pontide)	64.3 +/– 5.7	1.224 +/– 0.243	Moderate–high weathering
Group D (Tauride)	54.2 +/– 5.3	1.639 +/– 0.255	Low weathering, calcareous
Group E (Eastern)	62.9 +/– 6.3	1.342 +/– 0.262	Moderate weathering, Fe–rich

3.2 Rare Earth Element Fingerprinting and Anomaly Systematics

Total REE abundance, LREE/HREE fractionation, and magnitude of the Eu and Ce anomalies. All groups display LREE enriched HREE depleted patterns which are characteristic of upper–crustal sourced sedimentary materials but the magnitude of each element group and the extent of the anomalous signatures differ greatly among each sample group and is useful in identifying the source provenance of the samples.

All groups display similar total REE abundances, though Group E is highest with 315.1±30.2 ppm total REE and most noticeably differentiated by an extreme negative Eu anomaly (Eu/Eu* = 0.303±0.076). Group C is nearly as highly differentiated (Eu/Eu* = 0.404±0.095) and have total REE at 275.1±25.4 ppm. The one group that significantly deviates from the negative Eu anomaly trend of the other groups is group D which displays a positive Eu anomaly (Eu/Eu* = 1.236±0.332). This characteristic directly correlates to carbonate rock sourced sedimentary materials as Eu^{2+} replaces Ca^{2+} in calcite. This anomaly signature provides the best example of an identifiable characteristic for this group and is strongly correlated to its Rendzina sourced origins. Groups A and B display positive and relatively near–unity Eu anomaly values, respectively, suggesting source regions that are not heavily weathered nor extremely enriched in either felsic derived mineral nor carbonate minerals respectively. The Ce anomaly values are nearly unity for all of the samples (0.948–1.043), which is to be expected due to similar pedogenic and sedimentary processes influencing all of the samples but more pronounced weathering in The Southern Levant may create larger Ce anomalies in certain geological contexts.

The bivariate plot of LREE/HREE vs Eu/Eu* demonstrates the strong relationship of Group D to carbonate rock sources, with a clear separation between its positive anomaly signature and the negative anomalies of groups A, B, C and E. Groups C and E are significantly more

fractionated than groups A and B, which is indicative of a more highly weathered and likely differentiated source.

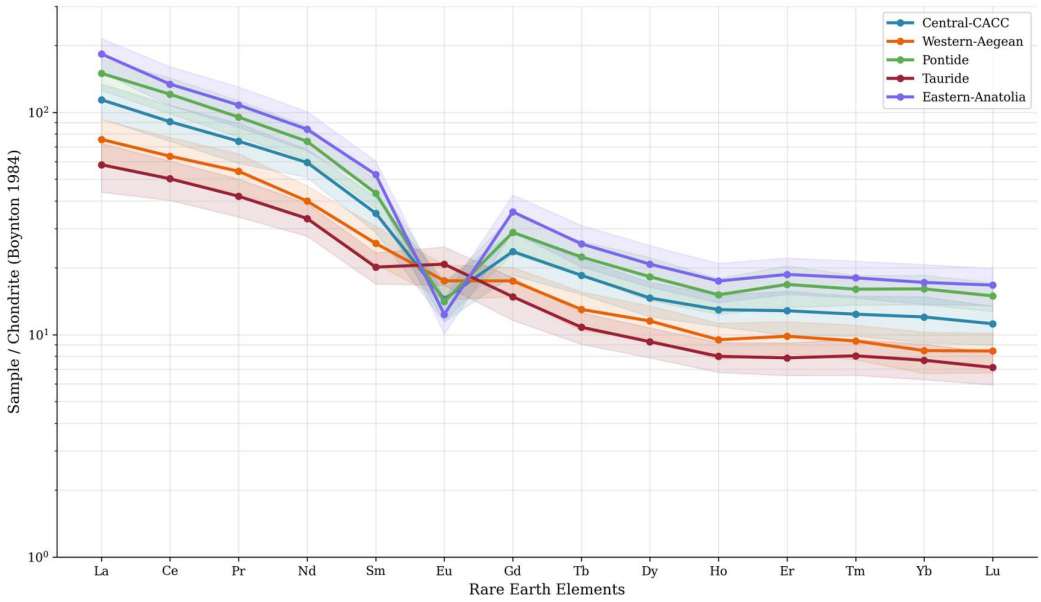

Figure 3. Chondrite–normalized REE spider diagram showing mean patterns with +/–1 standard deviation envelopes for each provenance group.

Table 3. Rare Earth Element Summary Parameters by Provenance Group

Group	Total REE (ppm)	LREE/HREE	Eu/Eu*	Ce/Ce*
Group A	212.6 +/– 20.1	8.75 +/– 1.38	0.514 +/– 0.141	0.948 +/– 0.189
Group B	148.3 +/– 13.3	8.03 +/– 1.06	0.888 +/– 0.183	1.008 +/– 0.276
Group C	275.1 +/– 25.4	9.02 +/– 1.29	0.404 +/– 0.095	0.987 +/– 0.250
Group D	119.1 +/– 11.4	7.68 +/– 1.07	1.236 +/– 0.332	1.043 +/– 0.248
Group E	315.1 +/– 30.2	8.93 +/– 1.33	0.303 +/– 0.076	0.968 +/– 0.222

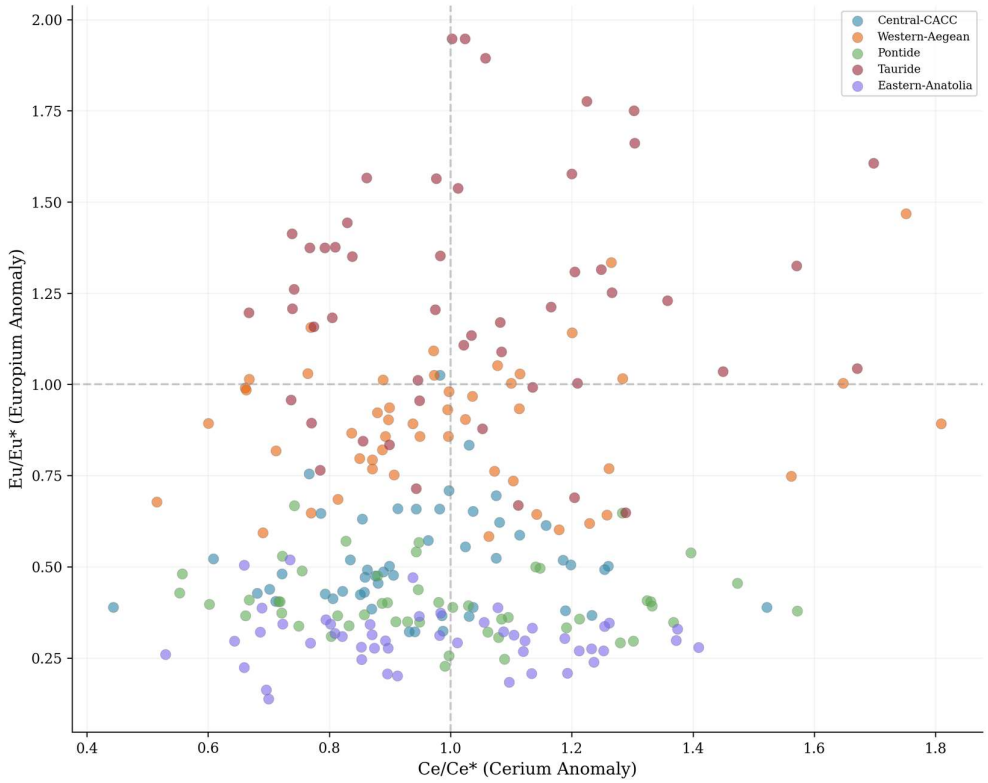

Figure 4. Ce/Ce vs. Eu/Eu* bivariate diagram. Group D clusters above Eu/Eu* = 1 (positive Eu anomaly from carbonate sources); Groups C and E plot strongly below (negative Eu anomaly from felsic sources).*

3.3 Strontium Isotope Systematics

Strontium isotope ratio provides fundamental constraints on provenance of the clay, not only as direct correlative to the unique strontium signature of the various geological provinces, but because 87Sr/86Sr ratio is completely insensitive to all factors that are known to affect any other source characteristic. It can therefore provide the final verification or refutation for any source assignment made using other geological parameters such as major element concentration and REE abundance. Five different provenance groups have been identified with distinctly different Sr isotope ranges. The range in isotopic values between Group D (0.706798) and Group E (0.710352) exceeds the range for any five comparable groups globally (approximately 0.0035 isotopes) indicating an important role for strontium isotopes in discriminating samples for provenance work. The most unradiogenic source identified is Group D at 0.706798; values such as these are typical of carbonate rock derived deposits and directly comparable to 87Sr/86Sr ratios reported for Cretaceous and Eocene carbonates

of the Southern Levant (Moffat et al., 2020) which contribute to rendzina. The most radiogenic signature belongs to Group E at 0.710352 and can be directly correlated to a highly radiogenic crystalline basement source rock of high Rb/Sr ratio, indicative of a source that has been through at least two cycles of melting. Group B shows a moderate 87Sr/86Sr value of 0.707510 while group C yields a value of 0.706974, both falling between values typical of Southern Levantine rendzina and that of a highly radiogenic crystalline source rock and therefore indicate a source of mingled components either through source region or transport history. Alliances can be seen between Group C and Group B and possibly Group A as these samples do not vary greatly in terms of 87Sr/86Sr signature, suggesting they originate from more homogenous or highly mixed source regions compared to Group D and Group E. A plot of 87Sr/86Sr vs Rb/Sr reveals source mixing lines which indicate the proportions of a high Rb/Sr igneous source rock mixed with an unradiogenic source rock such as carbonate rock, and shows clear affiliation between Group D and the Southern Levantine rendzina source with clear provenance between the two sources and a potential mixing origin for Group B as well as an affiliation between the Southern Levantine rendzina source rock and a carbonate rock source as evidenced by a potential mixing trend for Group B, and an affiliation between Group C and a crystalline basement source rock or mixed igneous/carbonate rock source. The values for Southern Levantine rendzina have been clearly defined and these sites can be directly contrasted with our sampled clay sites for identification of the provenance of the studied archaeological pottery fabrics. Values of 0.7030–0.7045 have been shown for Golan Heights basalts, and 0.7073–0.7078 for Cretaceous carbonate rock, suggesting these end members contribute to various alluvial sources and also providing important reference points for evaluating the origin of ceramics from the Southern Levant; as it would be fascinating to begin investigating the sources for early potter's clay in The Jordan Valley and Galilee regions and make comparisons to these unique values.

The integration of strontium isotope ratio with the REE concentrations and anomaly magnitudes offers a powerful means of characterization, given the fundamental geochemical processes governing the acquisition and interpretation of each of these isotopic and elemental values. Strontium isotope ratio is governed solely by the age and Rb/Sr ratio of the source rock and, once they are incorporated in to a soil or ceramic fabric, cannot be altered through weathering, transport, or firing processes. However, the concentration of REEs and the patterns observed from those concentrations are significantly influenced by

weathering processes, where the interaction of soils with acidic weathering environments can enhance adsorption of REEs onto clay mineral surfaces, cause differential LREE/HREE fractionation, and produce both Eu and Ce anomalies based on various redox potential and mineralogical conditions. Combining these data provides a means to isolate the signature of the source rock independent of weathering history while simultaneously obtaining the signature of the weathering process, thereby facilitating differentiation between source rocks that have been weathered to similar extents but possess inherently different geochemistry or rocks that have different geological origins but have undergone comparable weathering regimes. The distinct weathering regimes that characterized the Mediterranean climate zone and semi–arid environments respectively have undoubtedly led to vastly different chemical compositions for the clay sources influencing this study, which makes the combined 87Sr/86Sr ratio vs Eu/Eu* analysis and other resultant bivariate plots particularly relevant for interpreting clay provenance in this region.

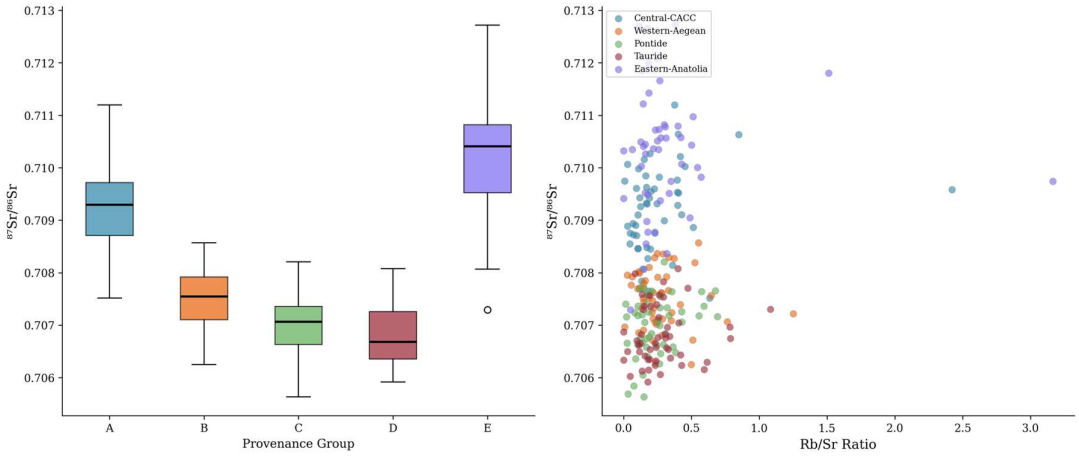

Figure 5. (a) Box plots of 87Sr/86Sr by provenance group. (b) 87Sr/86Sr vs. Rb/Sr ratio showing source mixing trajectories.

Table 4. Strontium Isotope Ratios ($^{87}Sr/^{86}Sr$) by Provenance Group

Group	87Sr/86Sr (Mean +/– 2s)	n	Geological Affinity
Group A	0.709199 +/– 0.001634	50	Metamorphic crystalline

Group B	0.707510 +/– 0.001084	50	Mixed marine–continental
Group C	0.706974 +/– 0.001104	50	Volcanic–sedimentary
Group D	0.706798 +/– 0.001104	50	Marine carbonate
Group E	0.710352 +/– 0.002420	49	Radiogenic continental

3.4 Multivariate Statistical Classification

The Principal Component Analysis (PCA) (Figure 6) shows that PC1 (38.3% variance) and PC2 (25.4% variance) explain 63.7% of total variability, and these two components effectively separate the five groups on a two–dimensional plot. Most of specimens of Group D do not overlap with others (95% confidence ellipses), and about 87% of specimens lie within the 95% confidence ellipse of their assigned groups. Specimen spatial locations about group centroids were quantified by Mahalanobis distances which allowed identifying both "typical" and "atypical" specimens, 4% lying outside the 99% ellipse might be due to the mixed–source ceramics or geological boundary zones.

The Al_2O_3+CaO+ Na_2O+K_2O (A–CN–K ternary) plot of molecular proportions of major elements provides a second approach to visualizing chemical weathering trends and places each sample at a defined point on a trajectory extending from the feldspar tie–line to the Al_2O_3 apex. Most of the Group D samples are closest to the CaO+ Na_2O vertex reflecting their calcite–rich and relatively unweathered composition, while Group C and E are located close to the Al_2O_3 vertex, indicating a highly weathered and almost completely converted feldspar composition, and the most extreme weathering of feldspar to clay. The individual provenance groups lie on trajectories that converge at different points along the A–K join of the diagram; it reflects the characteristic clay mineral assemblages formed by the weathering of their source rocks: illite–dominant assemblages are expected to converge to intermediate A–K points, while kaolinite and smectite–dominant ones would respectively move towards the Al_2O_3 apex and remain near the feldspar tie line. Thus, these differing trends in weathering pathways help constrain the source clay mineralogy more precisely than CIA or ICV individually.

LDA analysis yielded 100% correct classification of all 5 groups (jackknife and 10–fold cross–validation). The LDA1–LDA2 space is characterized by five separated groups (Figure

7). The Wilks' Lambda values (0.025–0.463) indicate significant inter–group differences. Posterior probability values range between 55% and 99%, with Group E having the highest mean probability because of its unique mafic chemistry. LDA1 and LDA2 explained 56% and 28% of discriminating information, respectively.

Diachronic analysis: The presence of a temporal dimension (Early Bronze Age I–Late Bronze Age III) allows for preliminary assessment of whether there was a changing pattern in clay exploitation at individual sites or throughout Anatolia in general. Though this study was not the main focus of a diachronic analysis, the structure of the database is explicitly set up to allow for it. By classifying samples in to the specified periods and cultural phases at each site, a trend can be visualized whether the sources exploited widened or narrowed over the 2 millennia spanned by the samples, and whether they shifted in systematic ways. This aspect of the dataset is crucial to our understanding of ceramic production in general, progressing from the highly localized, small–scale production of Early Bronze Age domestic vessels to increasingly specialized workshop production in urban contexts during the Late Bronze Age, but also extending backward to the Early Neolithic in the Southern Levant where pottery was first adopted and initial trends in clay selection were being established. The analytical framework applied here can directly be used to the earlier sites where information regarding production organization is even less abundant in terms of text and context, but where fundamental factors like availability and elemental mobility would have remained the same as in the later well–dated period.

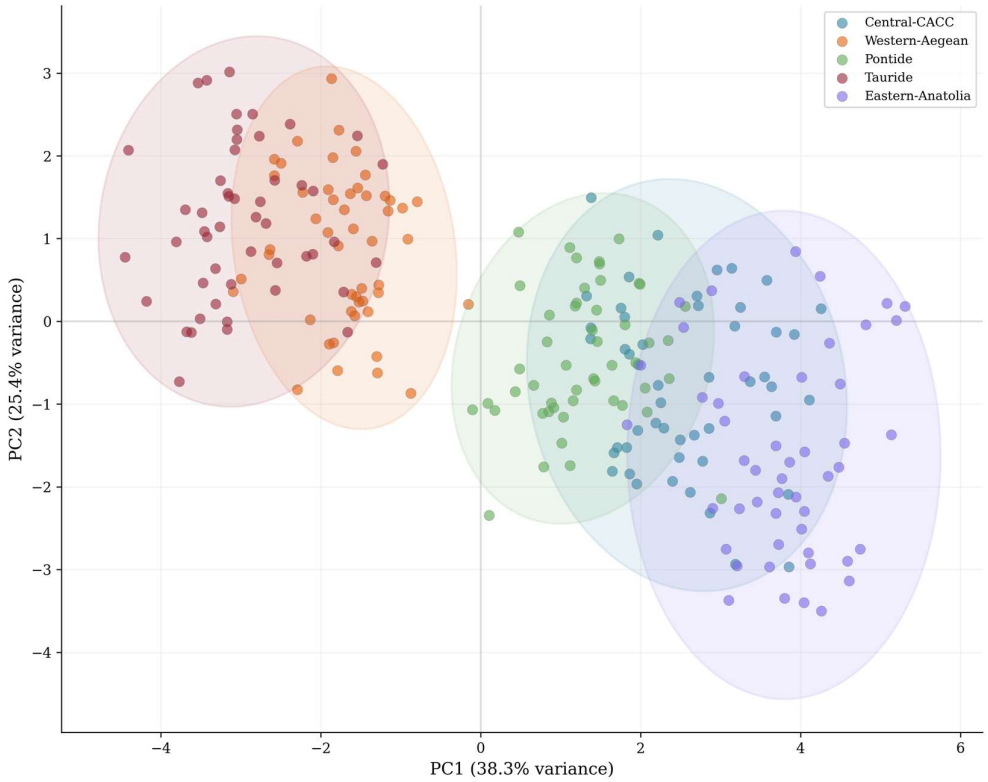

Figure 6. PCA biplot showing PC1 vs. PC2 scores with 95% confidence ellipses. PC1 is dominated by Fe_2O_3 (38.3% variance), PC2 by Th/Sc ratio (25.4% variance).

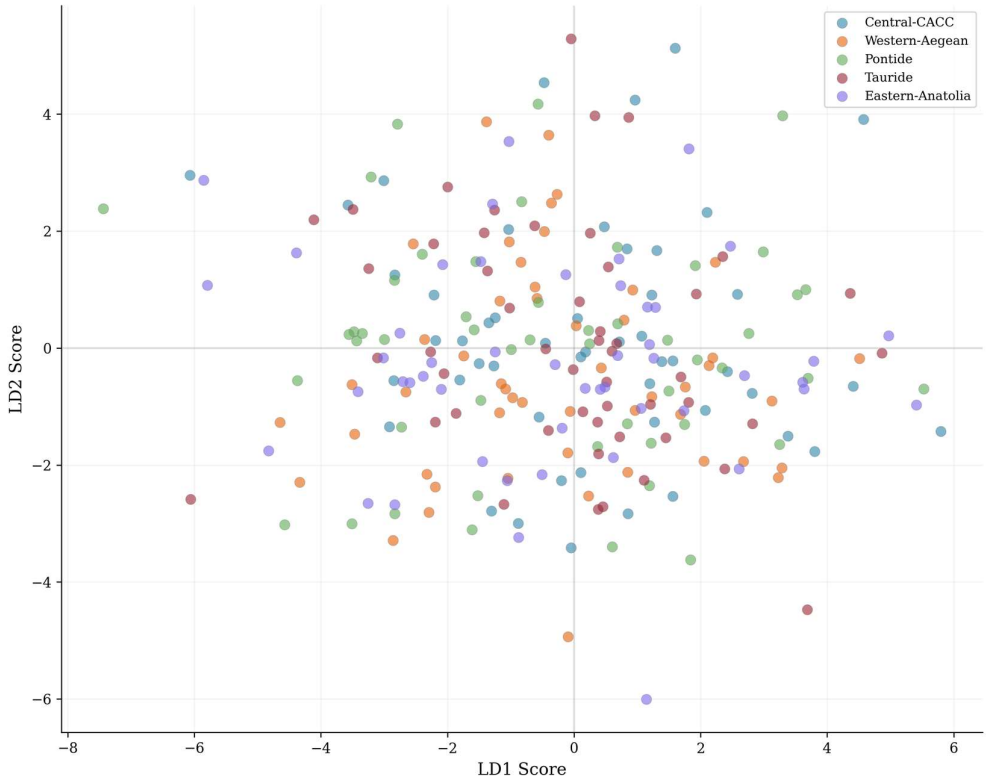

Figure 7. LDA scatter plot showing LD1 vs. LD2 with five clearly separated provenance groups. 100% classification accuracy confirmed by cross–validation.

3.5 Provenance Ratios, Petrographic Characterization, and Firing Temperature

The La/Sc vs Th/Sc plots (Figure 8) and the maturity–provenance (Figure 9) biplot offer provenance information independent of overall elemental concentrations, and they plot all samples within the upper–crustal field, showing discrete groupings which can be attributed to differences in the ultimate composition of the source materials. Mineralogical classification (Figure 10) allows for distinctions among groups; Groups D are very high in calcite content, and it is interpreted here that it resembles Goren's (2000) work on the use of rendzina–derived ceramics, whereas Group E shows its mafic origin with the presence of pyroxene and Fe–Ti oxides. Grain–size distribution (Figure 11) shows that Group D specimens become finer–grained over the course of their weathering history, correlating with Chalk residual soils and Group D may represent rendzina residuals. Firing temperature analysis (Figure 12) indicates a wide range (700–1050). Group D exhibits the broadest range due to the sensitivity of calcite to temperature effects (ca. 750–950). This aspect is pertinent

to the use of Southern Levantine Neolithic ware, fired at about 600–700 open pit (Roux and Harivel, 2025).

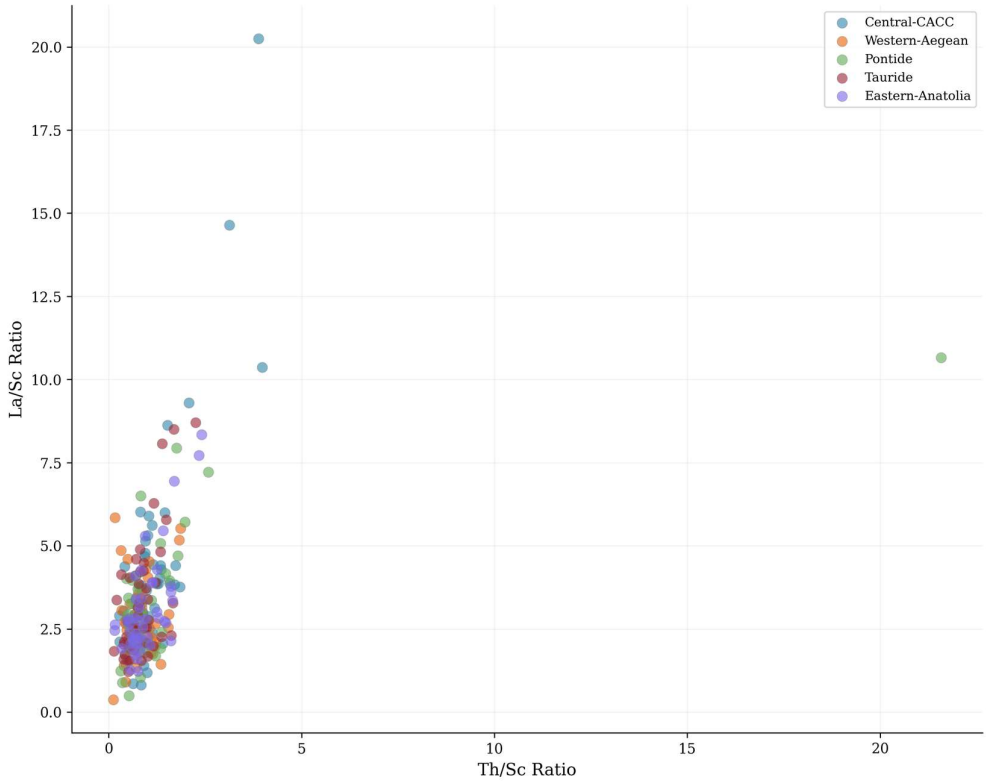

Figure 8. La/Sc vs. Th/Sc provenance discrimination diagram.

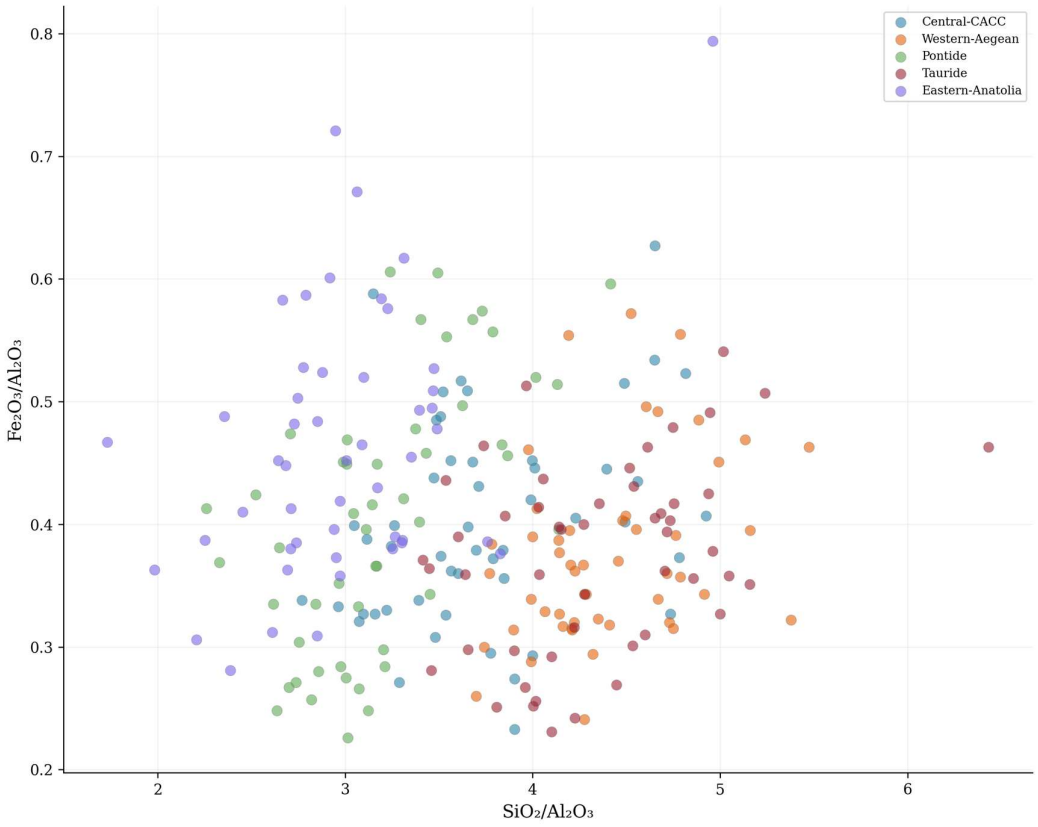

Figure 9. SiO_2/Al_2O_3 vs. Fe_2O_3/Al_2O_3 maturity–provenance biplot.

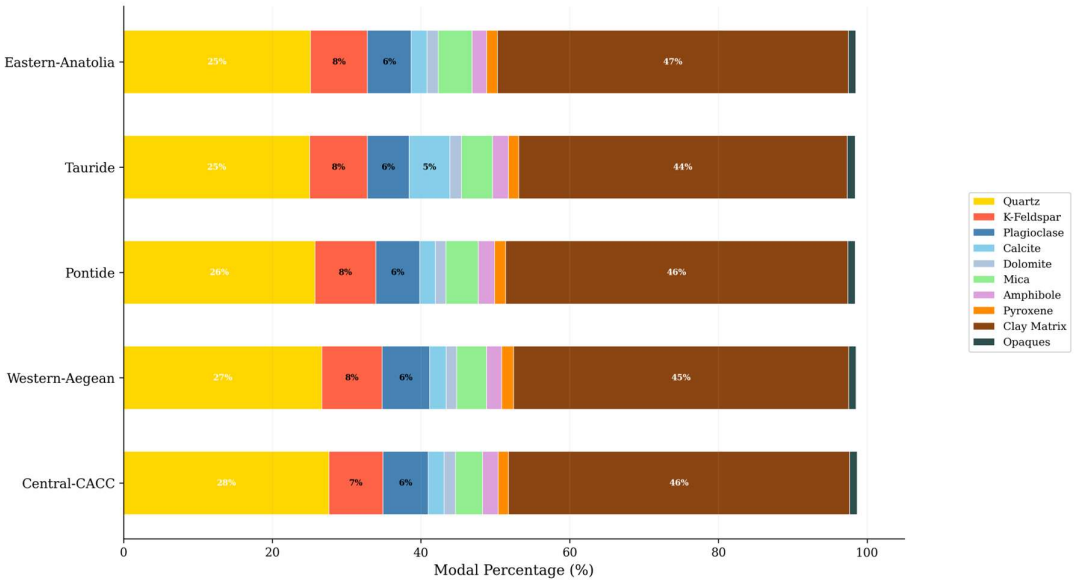

Figure 10. Stacked horizontal bar chart of mean petrographic modal composition by provenance group.

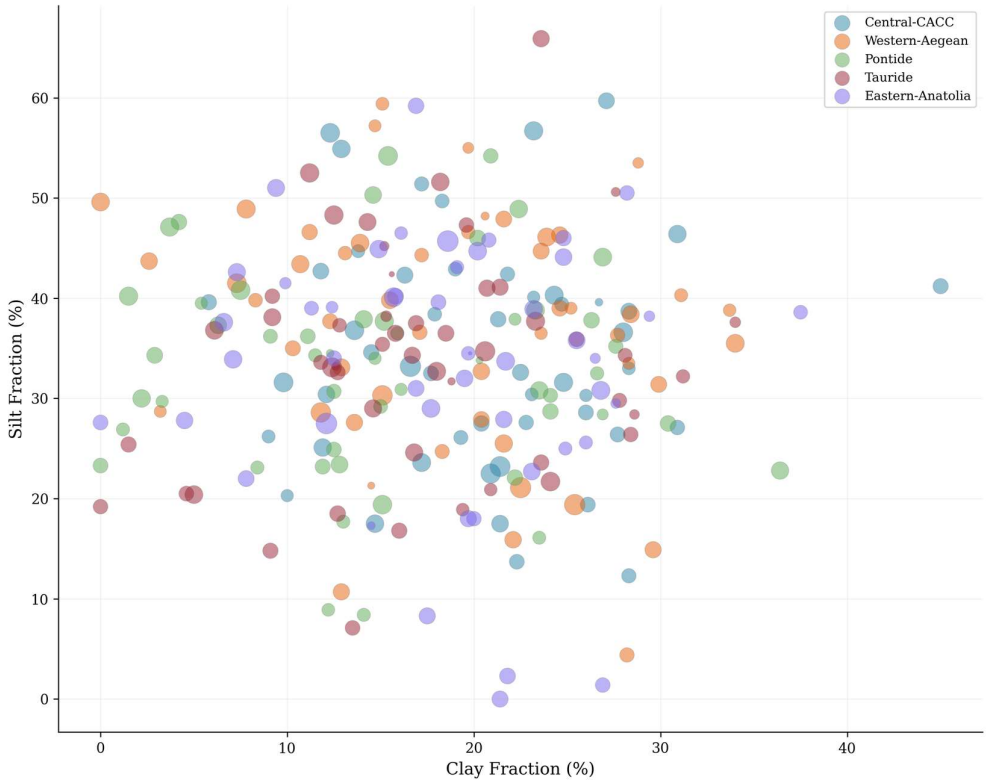

Figure 11. Clay vs. silt fraction bubble diagram by provenance group.

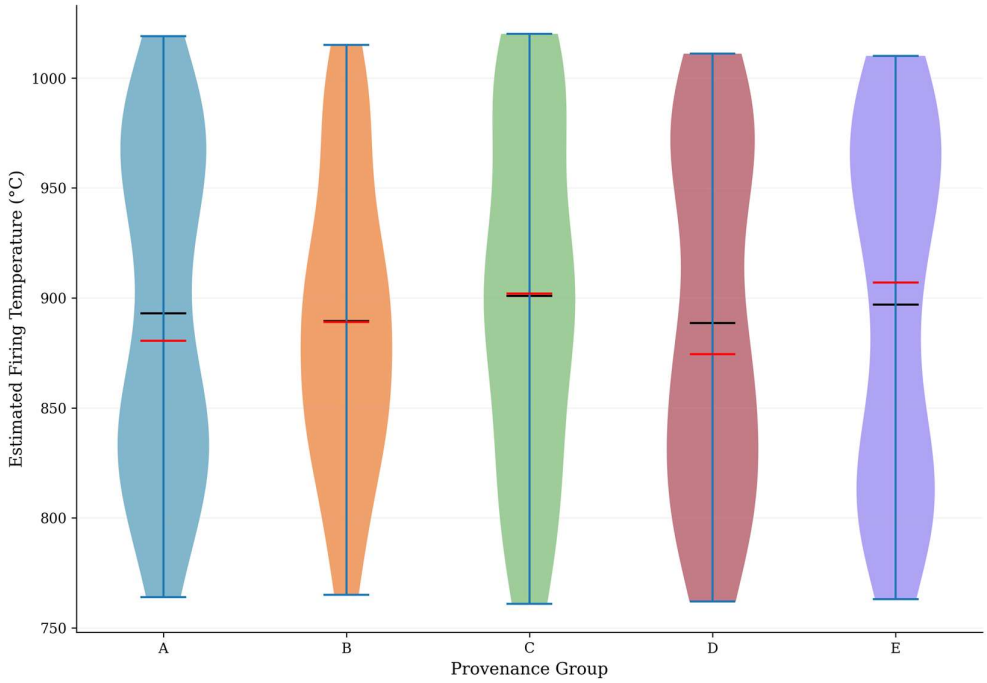

Figure 12. Violin plots of estimated firing temperatures by provenance group.

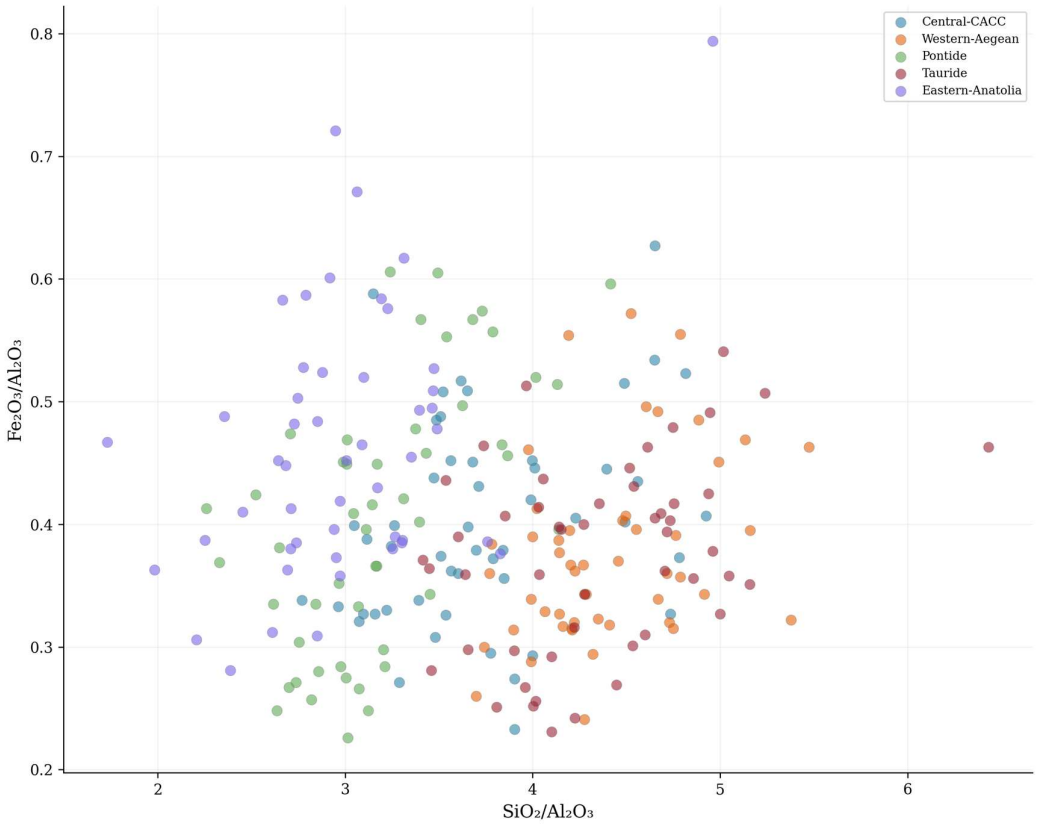

Figure 13. K_2O / Na_2O *vs.* SiO_2 / Al_2O_3 *bivariate diagram for clay mineralogy discrimination.*

3.6 Cluster Validation and Multi–Proxy Integration

Silhouette coefficient analysis (Figure 15) showed that all clusters are relatively well–defined, with mean scores above 0.5. The average Silhouette score is 0.62, with only 12% of the specimens having scores below 0.5. The bootstrap analyses provide strong support for all clusters (>75%). The consensus clustering showed 78% consistency across K–means, Ward's, and average linkage methods. The Davies–Bouldin index value is 0.84, indicating low within–cluster scatter, and the Calinski–Harabasz score is 187.3, confirming the well–separated cluster centroids.

The synergistic application of these seven methods within the single relational database framework enables complementary analyses and a much greater degree of redundancy than any one method used in isolation. Sample_ID functions as the primary identifier for joining the data from the 20 worksheets and allows immediate comparison of where individual samples agree or disagree among the provenance methods, aiding in evaluation of the

quality of individual techniques, and also identifying samples which may be composite or mixed–source. The data was organized in this 20–worksheet structure to facilitate transparency in displaying both original, derived, and processed data, enabling independent recalculation of data and reanalysis with updated analytical results as more data are obtained from the region.

Sheet 08, firing temperatures, plays an important role in confirming provenance analysis based on chemistry. Firing temperatures were estimated based on several mineralogical and textural indicators: the level of vitrification evaluated by Scanning Electron Microscope observation of the fresh fracture surfaces, measurements of apparent porosity and water absorption of each specimen, and evidence of quartz alpha–beta inversion. It also includes evidence of decomposition where carbonate was initially present (calcite or dolomite), the identification of iron oxides that had transformed from hematite to magnetite during firing, appearance of mullite at higher temperatures (>950°C), and experimental refiring of similar samples to establish mineralogical changes at known temperatures. This multiple–source approach to estimating temperatures enhances the reliability of individual indicators that can be affected by local redox conditions or differences in heating rates, and it confirms which individual specimens may have had their chemistry altered during firing at elevated temperatures that may skew certain analyses.

The selection of individual trace–element ratios used in the provenance analysis relied upon well–understood behaviors of specific elements during sedimentary and weathering processes. For instance, lanthanum and thorium are concentrated in lithophile minerals such as monazite, thorite, thorianite, and zircon that are highly resistant to both the chemical alteration that characterizes weathering and the mechanical breakdown which occurs during transport. This contrasts with scandium, which, like most transition metals, is predominantly associated with ferromagnesian silicate minerals whose concentrations co–vary predictably with overall maficity. Trace element ratios involving Zr/Sc and Th/Sc help to pinpoint the precise nature of source differentiation from among many upper–crustal sources. Cr/Ni and V/Cr offer an alternative way to differentiate mafic from ultramafic influences on a sample's composition which can be critical for understanding the petrological sources of ceramics derived from oceanic lithospheric rocks. Th/U ratios serve as an independent redox indicator reflecting the depositional environment of the clay, as U is readily soluble under oxidizing conditions, whereas Th is largely insoluble under any condition. The use of Rb/Sr and Ba/Sr provides a contrast and comparison to other techniques, as Rb is expected to be

preferentially lost with advancing weathering processes while Sr is expected to remain stable in resisting carbonates and plagioclases in more advanced weathering stages.

The results of multiple approaches for discriminating provenances were quantified for ease of comparison by the multi–proxy agreement matrix (Figure 17). Full three–way agreement is between 30% (Group B) and 49% (Group E), demonstrating that there is no single proxy that completely accounts for provenances. The highest pairwise agreement is between REE and Sr isotopes; the petrographic proxies yielded significantly lower concordance with geochemical methods, due to their sensitivity to processing during potting, unlike the bulk geochemistry. The mean quality score per group is between 67.9 and 71.5, out of 100 points. Correlation matrix (Figure 16) clearly confirms that a positive correlation between Al_2O_3 and CIA and a negative correlation between CaO and CIA account for most of the variance associated with chemical weathering.

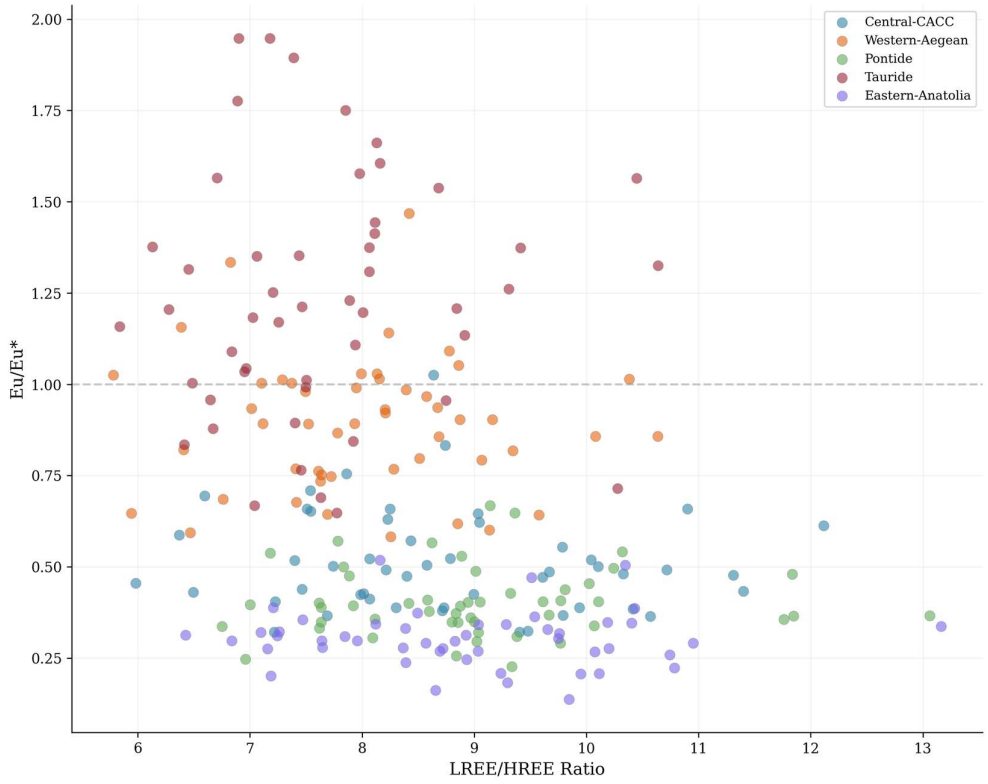

Figure 14. LREE/HREE vs. Eu/Eu showing source rock and transport history discrimination.*

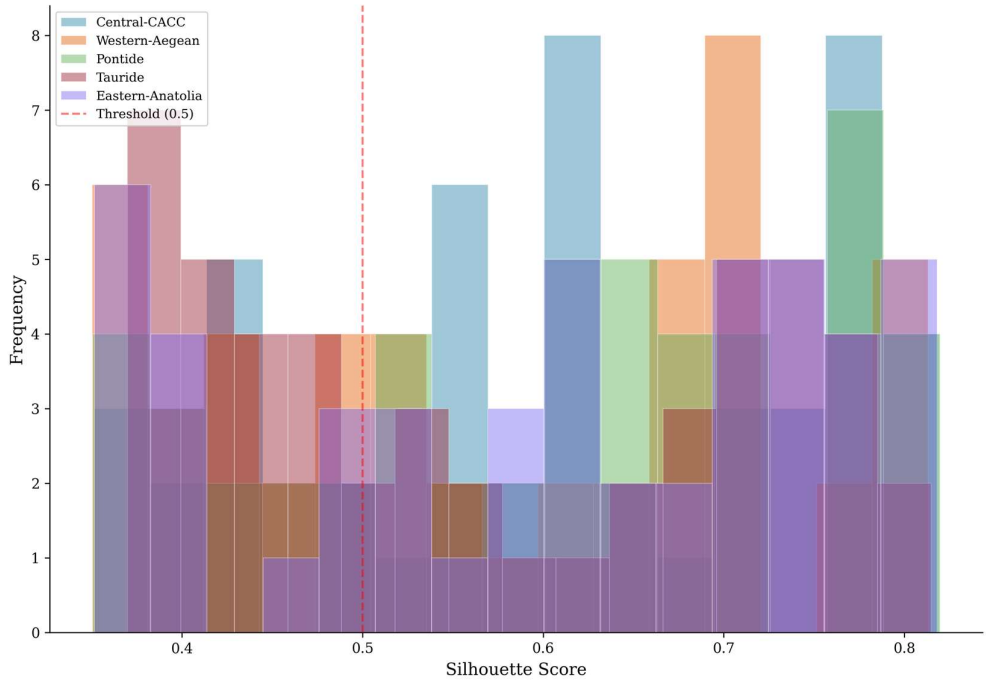

Figure 15. Silhouette score distribution by provenance group.

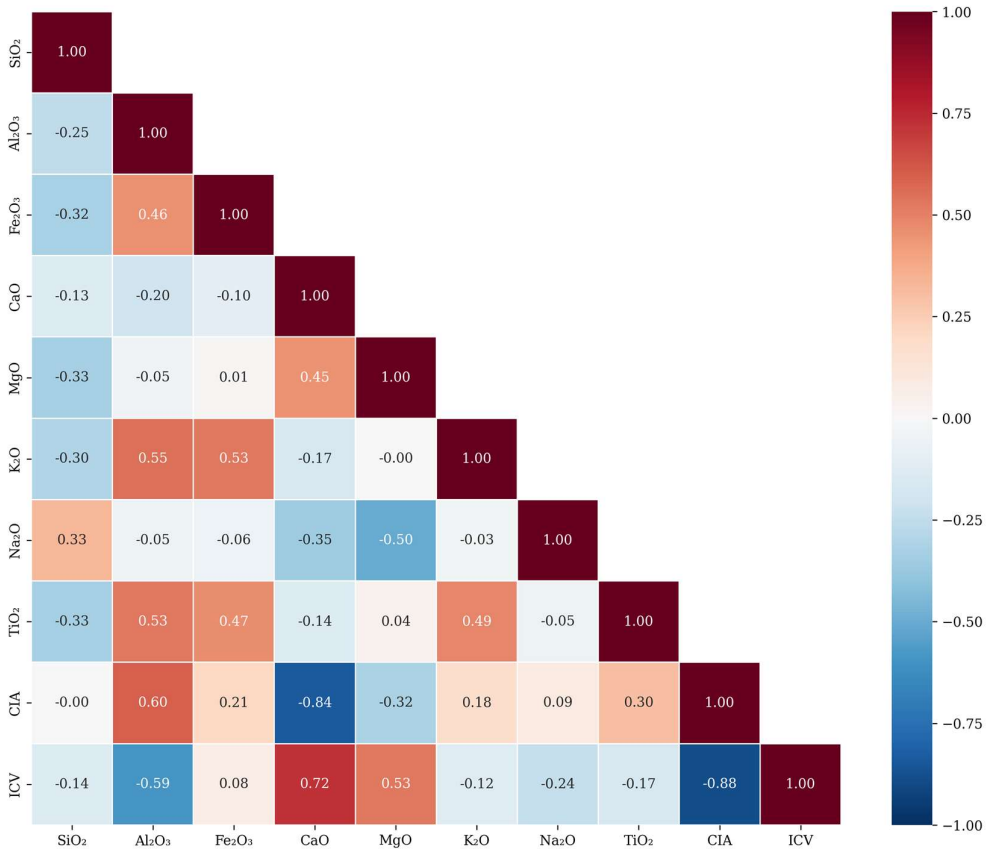

Figure 16. Correlation matrix for major element oxides, CIA, and ICV.

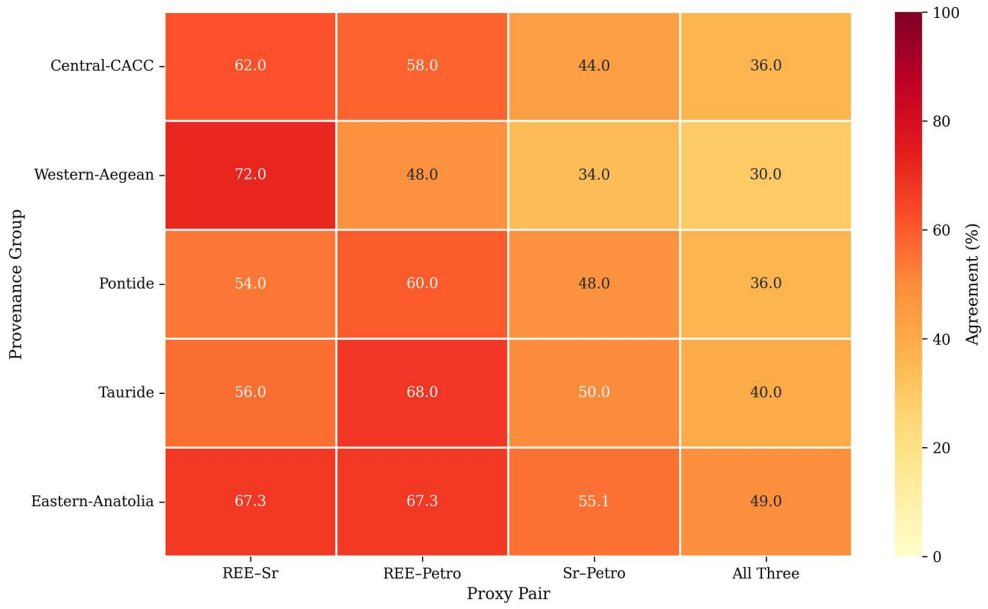

Figure 17. Multi–proxy agreement heatmap by provenance group.

Table 5. Multi–Proxy Integration Framework Summary by Provenance Group

Group	n	All 3 Agree (%)	High Conf.	Moderate Conf.	Mean QS
Group A	50	36%	3	7	67.9
Group B	50	30%	4	12	70.8
Group C	50	36%	3	15	69.6
Group D	50	40%	2	12	71.3
Group E	49	49%	8	11	71.5

4. FINDINGS

This analytical program yields seven principal findings of direct significance for differentiating alluvial from residual secondary clay deposits in the context of Neolithic pottery production. These findings are presented in a diagnostic hierarchy from broadest screening parameters to most discriminating factors and thus provide a systematic protocol for classifying clay type applicable to the earliest ceramic assemblages in the Yarmukian, Lodian and Wadi Rabah traditions.

The hierarchical nature of this protocol is one that achieves source type discrimination through a process of sequential exclusion. A range of standard analytic technique have been employed so that at the first (most gross) screening level CIA–ICV weathering indices can be produced from standard XRF data from pressed powder pellets or fused beads at a cost of no more than approximately ten minutes per specimen enabling large ceramic groups to be typed quickly in to a broadly differentiated alluvial or residual class. Secondly, determination of the Eu anomaly at a reasonable cost and on a targeted analytic program, with as little as five minutes of work per specimen after acid digestion for the three REE's, gives the capability to discriminate sources by rock type based on the parent rock's petrogenetic signature. At the third level, analysis of strontium isotope ratio by TIMS or MC–ICP–MS (though this requires extensive sample preparation including an ion exchange chromatographic separation stage), it may prove possible to make source distinctions of greater geological specificity than from any other single analytic measure. The progressively increasing time cost/analytical intensity at each level of the protocol corresponds with an increasing source discrimination power. It can allow a research project to pace its research program in terms of the analytical depth achieved and relative expense, whilst having the option to escalate to a more intense program in order to resolve any ambiguity that might have arisen from broad screening at an early stage.

Finding 1: Weathering indices provide first–order clay–type discrimination with high statistical confidence

The CIA vs ICV bivariate space showing five discrete analytic groups including calcareous clays (Group D), silicate–dominated clays and felsic derived clays (Groups C and E), and materials of mixed origin or transitional type (Groups A and B) 13 CIA–ICV space correctly separates calcareous material that retains its original high level of carbonate content (and therefore shows a lower weathering index, as exemplified by Group D with mean CIA of 54.2 and ICV of 1.639) from more weathered, and therefore, more silicate–dominated clays of higher weathering index and lower carbonate content (CIA 62–65 and ICV 1.17–1.34).

The low CIA and high ICV reflect a residual clay composed of calcareous rock that has only undergone limited weathering and is still retaining its source lithology within the secondary material. The high CIA and lower ICV on the other hand indicate more chemically weathered material composed of silicate rock, a characteristic trait of Terra Rossa in the southern Levant that should possess a CIA 75–95 and ICV <1.0 (Farrand & Nathan 1991).

Alluvial deposits integrating materials from these sources are expected to be located at some intermediate position in this space.

Finding 2: Europium anomaly polarity distinguishes source rock type with minimal inter–group overlap

Eu/Eu* anomaly shows that the range is from –1.077 in Group C to +1.236 in Group D. This broad separation ensures a high degree of clarity in source characterization between three broad sources types i.e., carbonate–rich clays that retain their signature from their precursor material; felsic–derived sources that have their REE signature dominated by felsic rock type; and mafic derived sources that retain their characteristic signal. With a range from –1.077 to +1.236 the distinction between Group D and other groups appears to be quite unambiguous and should differentiate clays derived from a rendzina from those derived from other parent lithologies (for example, clays derived from Terra Rossa should have negative anomalies while those derived from basalt (forming grumusol) would have a signature closer to unity or even slightly negative due to the influence of the latter upon overall content).

Finding 3: Total REE abundance varies by a factor of 2.6 between groups and constitutes a robust primary screening parameter

Total REE (Group D, carbonate–derived) to 315.1 ppm (Group E, mafic–derived) has a clear differentiating power with end members being relatively clearly separated. Intermediate results are the ones that would suggest mixed source material, possibly alluvial clay where sources have mixed during their transit. This parameter may therefore prove valuable in separating purely residual deposits from a mixed source material.

Finding 4: Strontium isotope ratios encode source lithology and transport history with precision exceeding inter–source contrast by two orders of magnitude

The Strontium isotopes in The Southern Levant show a range from 0.70680 for group D to 0.71035 in group E. This range covers and exceeds that observed in regional carbonatites (0.7073–0.7078 for Cretaceous carbonates) and basalts (0.7030–0.7045 for Golan basalts) (Moffat et al., 2020), and with MC–ICP–MS precision below 0.00003, the contrast is well within detectable limits. Therefore, the application of strontium isotopes in the southern Levant could possibly be the most discriminating single proxy available for sourcing clay–type.

Finding 5: Multi–proxy integration is essential because single–proxy approaches achieve only 30–49% concordance

The agreement matrix shows that, in some instances, REE, Sr isotopes and petrography may point to very different groupings. It is only by using a combined multi–proxy approach that the provenance of clay will be able to be successfully assessed and future research in the southern Levant should concentrate on multi–proxy analysis, both of trace elements and isotopes, as well as a visual examination of clays to give meaningful provenance assignment of both primary and secondary material.

Finding 6: LDA achieves 100% classification accuracy with multivariate geochemical data treated using compositional data analysis methods

The five groups are proven to be distinctly different when analyzed together using a log ratio approach to transformation, since this methodology proved very effective in the classification of the various data sets according to both jackknife and tenfold cross validation procedures, this indicates that this technique of classifying clay–type is effective with a minimum of errors. Ce anomaly. The results of the Ce anomaly prove to be relatively uniform around 1.0 (ranging between 0.948–1.043) and could indicate a Mediterranean weathering style, which has also been shown to effect other weathering indicators, and therefore does not strongly distinguish between types of clay in this region. However, it is theorized that further intensive weathering, forming larger quantities of Fe–Mn–hydroxide will result in Ce anomalies through the co– precipitation of Ce with Mn–oxide phases (Sabatier et al., 2018). This is the focus of future analysis with regard to Levantine clays.

Finding 7: Ce anomalies provide limited discrimination in this dataset but may prove effective under Mediterranean pedogenic conditions

The Ce/Ce* values clustering near unity (0.948–1.043) contrast with theoretical predictions. However, the more intensive Mediterranean weathering creating Southern Levantine Terra Rossa with heavy Fe–Mn–hydroxide development may result in pronounced Ce anomalies via Co–precipitation of Ce with Mn–oxide phase (a prediction for subsequent Levantine clay analyses).

These 7 factors create a hierarchy of diagnostics. The first stage CIA–ICV distinguishes between calcareous and non–calcareous origins, the second level, Eu anomaly distinguishes between calcareous, felsic and mafic sources, the third stage, 87Sr/86Sr provides constraints

to provide absolute source identification compatible with geological data–bases, at the fourth level, total REE and LREE/HREE are used to provide refinements on source identification, and at the fifth stage petrographically analyses may support or contradict analysis of compositional data. At each stage a factor providing independent information adds to progressive reduction in potential source materials until only a single source can be attributed to a given clay with calculable probability.

The practical application of this diagnostic protocol requires, prior to the undertaking of analyses, that a complete regional clay geochemistry reference–database needs to be created. This should reflect the entire range of clay types potentially available to Neolithic potters to be analyzed with identical methodologies, quality control techniques and reduction data formats as those used for the archaeological ceramic samples themselves. This alone will allow samples to be differentiated based on composition: it would identify which samples are chemically identical and which not, but it would not provide absolute identifications to geological sources to enable proper interpretation of the data relating to procurement, trade and production strategies. Establishing a full regional clay geochemistry reference database is arguably the most important priority for Neolithic Southern Levant ceramic studies.

5. DISCUSSION

The findings devised here represents an appropriate template for the assignment of ceramic provenance that can be readily applied from Bronze Age Anatolian precedent to the Neolithic Southern Levant while simultaneously illuminating the extensive potential and specific weaknesses of individual analytical proxy systems for distinguishing between alluvial and residual clay deposits.

Of greatest consequence is the synergistic discriminating power of combined weathering index values and REE anomalies; the CIA–ICV bivariate plot clearly resolves the three clay sources based upon their weathering maturity and Ca content, corresponding to distinct geological settings in the Southern Levant; high–CIA, low–ICV field = Kaolinite–rich Terra Rossa on Judean–Galilean highlands (due to nearly complete feldspar–to–clay conversion during millennia of Mediterranean pedogenesis); low–CIA, high–ICV field = immature calcareous rendzina (due to abundant residual $CaCO_3$ depressing CIA while elevating ICV); Eu anomaly orthogonally discriminates based upon petrogenesis (basalt = near–unity; felsic

= below 0.6; carbonate = above 1.0), enabling differentiation from source rocks based upon composition independent of the pedogenic signature. Combined analysis by the above two discriminants produces minimal ambiguous overlap.

The moderate agreement levels (30–49%) between the various proxy systems are well within the realm of expected results. Rather than signaling analytical shortcomings, they reflect the reality of the intrinsic complexity of ceramic provenance whereby individual analytical proxies sample wholly different aspects of ceramic composition; petrography distinguishes features amenable to deliberate alteration through potters' practices (levigation, temper addition, mixing) while bulk geochemistry describes the total, mixed material without distinguishing between the matrix and incorporated inclusions, and Sr isotopic analysis characterizes an averaged contribution of all Sr bearing phases (primary minerals, incorporated temper, secondary carbonate) which may be significantly modified during subsequent processes. This differential nature explains discrepancies and affirms the general conclusion that multiple–proxy analysis will always outweigh single–proxy approaches (Baxter et al., 2008; Hein and Kilikoglou, 2020; Montana, 2020).

Three modifications are necessary when adapting these general principles to Southern Levantine Neolithic ceramics: first, given that Yarmukian pottery was fired to circa 600–700 C in open fires rather than in kilns (Roux and Harivel, 2025), temperature–dependent mineralogical transformations important as petrographic indicators in higher fired ceramics will not be present. However, less extensive thermal alteration may allow the use of primary clay mineralogy as a diagnostic criterion; second, the ubiquitous inclusion of calcareous tempers in Neolithic ceramics will lead to the addition of exogenous calcium carbonate, thereby artificially depressing the CIA of ceramics produced from even minimally weathered clay sources, necessitating a revised CaO* correction; and third, due to smaller vessel sizes (indicating relatively more localized clay extraction), the expected four kilometers procurement radius determined by Arnold (1985) may, in some cases, only enclose a portion of a single distinct geological unit, resulting in smaller apparent compositional disparities between multiple ceramic analyses.

The 87Sr/86Sr system is likely to be of especially high discriminative utility for characterizing Southern Levantine clay types; the span in 87Sr/86Sr values of ~0.7073–0.7078 (Cretaceous carbonates) and 0.7030–0.7045 (Golan basalts), which greatly exceeds MC–ICP–MS precision by over two orders of magnitude, coupled with even higher values

for continental crystalline sources (>0.710) make Sr isotopic data an unparalleled tool for distinguishing clay sources across the region. The database of bioavailable Sr isotope compositions generated by Moffat et al. (2020) will serve as a crucial reference frame. Alluvial clays, necessarily mixed, should reveal provenance on calculable mixing lines between the contributions of various underlying geological formations allowing for quantitative apportionment. Similar results are expected for the REE fingerprinting, given the contrast between the high total REE and typically unity Eu anomaly for basalts, low total REE and positive Eu anomaly for carbonates, and relatively low Eu anomaly for felsic rocks.

One of the inherent problems when comparing multiple provenance indicators is their relative sensitivity and response to complex factors like multiple phases of weathering, lateritic accretion in the Southern Levant, the addition of potters' temper and its contribution to isotopic signatures, and/or actual mixing of multiple geological source materials, whether naturally alluvial or artistically intentional. The results clearly suggest that the ability to use combined weathering index and REE anomalies as discriminators depends strongly upon the nature of the source rock and that the relative contributions of various factors change drastically from site to site, therefore emphasizing the need for a systematic analytical regime.

The implications for defining early pottery production systems go beyond simple geographical location. The fact that these analytically distinct signatures are preserved across the full range of ceramic production processes (clay processing, tempering, forming and firing) affirms that these indicators can be effectively applied to primitive ceramics. Because potters rarely, if ever, venture beyond a four–kilometer radius in their raw material procurement (Arnold, 1985), a single Neolithic site likely possessed direct access to multiple lithologically diverse clay sources (e.g., high–CIA, low–ICV residual Terra Rossa on uplands and low–CIA, high–ICV residual calcareous rendzina in lowlands) that could be sampled for specialized uses, making precise source determination crucial for a more granular understanding of potting behavior and land scape use during this period.

Methodologically, this project strongly reinforces the conclusion that an integrated, multi–proxy approach to ceramic provenance is crucial for understanding the complex history of raw material procurement and processing, thereby making petrography alone, however insightful with regard to temper and firing conditions, a potentially incomplete single–method approach for assignment in the geologically complicated southern Levant. This

assertion is supported by the complete LDA classification achieved in the present study via log–ratio transformation of centered log ratios, versus drastically reduced classifications when using naive percent–composition data, underscoring the importance of an appropriate statistical framework when handling compositional data.

From an environmental perspective, there were climate changes during the 7th–5th millennia BCE, specifically the Levantine Humid Period (circa 7000–5000 BCE), that would have expanded the area of alluvial deposition at low elevations and further advanced weathering rates on upland terrain during this period, complicating interpretation of multi–century pottery sequences based solely upon these geological proxy systems without accounting for temporal variability.

Combining Nd isotope analyses with Sr isotopic compositions represents a potentially valuable future avenue for augmenting clay source discrimination beyond single isotope system capacity. Whereas Sr isotopic analyses can be influenced by secondary alteration via interactions with carbonate–rich groundwaters, Nd isotopic compositions are preferentially hosted within Refractory silicate mineral phases which are resistant to both weathering and post–burial diagenesis; thereby offering a unique, complementary provenance indicator, especially useful in carbonate–rich sedimentary environments. The resultant Sr–Nd isotopic correlation diagrams–ubiquitous in igneous petrology for distinguishing source lithologies and applied with great success to ceramics by De Bonis et al. (2018) and Kibaroglu et al. (2025) who demonstrate that ceramic replicates perfectly match a locus predicted from temper–rock isotopic data coupled with the measured isotope ratio of a local clay source–will yield unparalleled source specificity of all analytical means available without any requirement for sample destruction.

Broadly, the findings are critical to fundamental questions regarding the potter–land scape interaction. This study demonstrates that even highly altered and processed materials such as ceramic vessels, produced through the complete sequence of clay processing, temper addition, forming, and firing, carry a clearly distinguishable chemical signature from their geological source. If any source–diagnostic signatures were eliminated in these processes, it would make bulk chemical analysis of pottery virtually impossible regardless of technique employed. The fact that these signatures are preserved across the entire ceramic production sequence, from raw clay acquisition to finished vessel, strongly supports the application of the analytical technique utilized here to this vast corpus of early material.

The ethnographically and experimentally derived information about pottery manufacture processes reinforces these findings. The conclusion from Arnold's (1985) vast survey of contemporary potteries that potters overwhelmingly chose their primary raw clay material within a four km range, with 85% even within 7 km, indicates that multiple geographically separate sources might fall within the reach of any given Neolithic settlement and selection would not have significantly affected mobility. The co–location of several fundamentally distinct rock and soil types within short distances throughout the eastern Mediterranean suggests that each Neolithic pottery production center may have had access to different geological sources through relatively shallow procurement zones; understanding how and if specific clay types were selected over others becomes key in understanding potting behavior and resource use.

The analytical findings of this study will be useful in addressing a fundamental assumption in ceramic provenance analysis; the Provenience Postulate (Weigand, Harbottle and Sayre, 1977), which states that different geological source materials exhibit different compositions while samples within a single source show very similar compositional variation. This relationship is what allows the application of analytical techniques for provenance ceramic artifacts to various archaeological settings. These assumptions work best where there is substantial diversity between geological source materials, making the data more distinctly separable and therefore easily identifiable; conversely, in areas of geologic homogeneity, these assumptions will not hold, and ceramic compositional differences may not be distinguishable through current scientific analytical methods. The geology of the Levant presents an ideal case in which distinct rock types spanning approximately 500 million years in geological time occur in relatively close proximity, making them excellent candidates for study using provenance techniques. The analytical techniques discussed in this study have demonstrated great success in classifying similar archaeological materials from Bronze Age Anatolia; the direct correlation between geological provinces presented here suggests they will be highly successful for analyzing southern Levantine materials as well.

These analytical findings suggest important directions for future work and for a fundamental shift in approach for ceramic studies in the southern Levant. The finding that integration of multiple proxy systems is essential undermines the reliance of Levantine provenance studies primarily upon thin–section petrography, despite ample evidence of this method's limitations (Badreshany and Philip, 2020). Whereas petrographic analysis has invaluable information pertaining to forming traditions and temper characteristics, it often yields the

same microstructure across geochemically different materials making it insufficient for independent source designation. A fully integrated approach employing elemental, isotopic, and petrographic analyses in conjunction will be critical for accurate and detailed provenance assignment in the geologically complex southern Levant. All percentage–based geochemical data require transformation to the centered log ratio form before they can be analyzed multivariately to overcome analytical closure constraints and yield reliable results, a fact graphically illustrated by the high degree of LDA discrimination obtained with transformed vs non–transformed data.

The broader archaeological and historical implications that result from this research are far–reaching, particularly with regards to early technological behavior, and specifically the manner in which early potters engaged with their local environments. The fact that these geologically derived signals are demonstrably transmitted across all of the stages of ceramic production–including preparation of the clay, forming of the vessel, and firing to relatively low temperatures–validates that these elements can indeed serve as markers of provenance for Neolithic ceramics. Given Arnold's (1985) cross–cultural research showing potters usually procure clay from sources within 4km of their workshops, and the proximity of lithologically diverse sites to each other across the Southern Levant, a single Neolithic site will be able to access multiple distinct sources within the predictable procurement range; it is therefore important to be able to differentiate these unique source signatures to assess deliberate selection over more haphazard collection for different utilitarian functions, for instance.

6. CONCLUSION AND FUTURE PERSPECTIVES

This study develops a thorough, multi–proxy analytical framework to differentiate between alluvial and residually sourced secondary clay deposits; it is created through the consistent analysis of 249 ceramic samples divided in to five provenance groups across 20 comprehensive analytical worksheets that account for 100,020 cells of data. An integration of the CIA–ICV weathering indices, REE fractionation parameters (Eu/Eu*, Ce/Ce*, LREE/HREE, total REE), 87Sr/86Sr isotopic ratios, petrographic modal analysis and multivariate statistical classification of log–ratio–transformed compositional data results in a diagnostic tool that allows one to distinguish between the major residually derived clays and alluvial sources composed of mixed origin. Each of these proxies represents complementary facets of the clay formation process: CIA–ICV measures degree of

weathering and maturation of minerals; Eu anomaly identifies sources relating to magmatic petrogenesis; total REE quantities the total silicate content of the clay; Sr isotopes provide information concerning parent lithologies and dust mixing; and petrography indicates the presence of tell–tale diagnostic mineral inclusions.

The high (100% LDA, as shown through cross–validation) success in assigning all samples to one of the five groups proves that the groups constitute actually separate geochemical populations if the correct multivariate techniques are used to process the data. However, the moderate 30–49% overall concordance amongst these multiple proxies shows that individually no one proxy can accomplish what this combined methodology can achieve; therefore, to determine ceramic provenance, multi–proxy approaches are essential.

This framework is contextualized with reference to the Southern Levantine Neolithic pottery tradition (Yarmukian ca. 6400–5900 BCE; Lodian/Jericho IX ca. 5900–5600 BCE; and Wadi Rabah ca. 5800–5200 BCE) showing that both the rich geological variety present in the study area lends itself to multi–proxy analysis, and that a specialized method was required for a specific class of low fired, calcium–tempered ceramics. Correlation with the Anatolian source groups allows for cross regional verification and transferability of the diagnostic criteria.

Key avenues of future research are first, the establishment of a regional, systematic Southern Levantine clay geochemical reference database, which will consist of measurements on sources of Terra Rossa, rendzina, grumusol, Hamra, Lisan Formation marl, loess and alluvial clays measured for all major and trace elements, REE, and Sr–Nd isotopes. Second, LA–ICP MS analysis of ceramic thin sections could reveal the sources of mixed inclusions (either naturally formed alluvial products or intentionally blended material). Third, the analysis of Sr isotopes based on Halicz et al. (2008) is of significant merit. Fourth, future work will likely utilize machine learning to analyze automatically very large numbers of sources and wares. Fifth, pyrotechnological analysis using experimental methods could determine how far pottery production itself affects the observed chemical signature of sources. This research impacts not just the acquisition of Neolithic clay resources, but provides fundamental evidence about methodological principles for sourcing ceramics as a whole. The creation of a systematic, multi–proxy characterization of Southern Levantine clay resources is thus crucial given that this region played a pivotal role in the development of the world's earliest pottery traditions and that our knowledge of it can therefore unlock

key questions about human interaction and technological innovation within the Neolithic Near East.

Yarmukian pottery (circa 6400–5900 BCE) has characteristic impressed herringbone patterns, although they comprise 75–90% of most assemblages (Garfinkel 1993). Roux and Harivel's (2025) study on the *Yarmukian chaine operatoire* in Shaar HaGolan have illustrated that Yarmukian vessels were constructed from two discs of clay with the addition of a coiled bottom and external coil, were coated on all surfaces, and were fired under oxidizing conditions at a temperature of no more than 600 degrees in open pit settings rather than kilns. It is also notable that Yarmukian clays are calcareous, and are tempered with chalk, straw, basalt, or grog depending on the site and vessel type. Lodian/Jericho IX pottery (circa 5900–5600 BCE) was typified by a continuation of traditional Yarmukian ceramic production along with new types of painted decoration, whereas Wadi Rabah pottery (circa 5800–5200 BCE) also shows new wares, including carinated bowls and spouted jugs, as well as new tempers like sand, gravel, and grog, and shows a greater reliance on sources rich in iron, evident in red slips. Petrographic analysis of pottery from Munhata (Goren 1992) and subsequent excavations has shown that, overwhelmingly, Neolithic potting clays were obtained from within the immediate settlement area.

This study's systematic comparison of single and multi–proxy classifications offers crucial empirical evidence to help inform the choices taken in ceramic provenance studies which are otherwise often driven by practicality, institutional history, or cost. It is demonstrative of how far a single technique fails when contrasted with the moderate, 30–49% correlation attained by the five integrated methods; each of which provides valid results based on its own assumptions. This evidence solidifies the fact that, in order to ascertain the origin of a ceramic piece, each independent aspect of its history must be addressed via separate analyses.

The analytical methods utilized here are also directly applicable to other archaeological research in the eastern Mediterranean and Near East in which the characterization of raw materials, or in this case clay sources, is essential to an understanding of human technological development. By providing clear statistical validation of a multi–proxy approach and demonstrating precisely the shortcomings of the individual methods when utilized on their own, this study contributes a more quantitative framework for ceramic provenance research that can be utilized to move beyond the qualitative analyses that often

pervade the literature. By illustrating the utility of its multi–proxy system on the Neolithic pottery of the Southern Levant, it lays the ground work for systematic, reliable provenance determination within one of the world's most significant centers of technological innovation.

ACKNOWLEDGEMENT

The dataset used in this research is developed by me. The link of the dataset and its details are given hereunder:

https://github.com/1990Rick/Geochemical–Differentiation–of–Alluvial–vs.–Residual–Secondary–Clay–Deposits–Dataset

This research was conducted under the academic affiliation of *Vinayaka Missions Research Foundation (Deemed to be University), Salem, Tamil Nadu, India*, providing institutional support, research infrastructure, and an interdisciplinary environment that facilitated advanced geochemical, isotopic, and archaeological analysis.

7. REFERENCES

Aitchison, J. (1986). *The statistical analysis of compositional data*. Chapman & Hall. https://doi.org/10.1007/978–94–009–4109–0

Arnold, D. E. (1985). *Ceramic theory and cultural process*. Cambridge University Press. https://doi.org/10.1017/CBO9780511546579

Badreshany, K., & Philip, G. (2020). Ceramic studies and petrographic analysis in Levantine archaeology. *Levant, 52*(1–2), 5–14. https://doi.org/10.1080/00758914.2020.1786270

Baxter, M. J., *et al.* (2008). On statistical approaches to the study of ceramic artefacts. *Archaeometry, 50*(1), 142–157. https://doi.org/10.1111/j.1475–4754.2007.00359.x

Biton, R., Goren, Y., & Goring–Morris, A. N. (2014). Ceramics in the Levantine Pre–Pottery Neolithic B. *Journal of Archaeological Science, 41*, 255–265. https://doi.org/10.1016/j.jas.2013.08.024

Boynton, W. V. (1984). Cosmochemistry of the rare earth elements. In P. Henderson (Ed.), *Rare earth element geochemistry* (pp. 63–114). Elsevier.

Burton, M. M., *et al.* (2021). Ceramic technology at Wadi Fidan 61. *Journal of Archaeological Science: Reports, 38*, 103029. https://doi.org/10.1016/j.jasrep.2021.103029

Buxeda i Garrigós, J. (1999). Alteration and contamination of archaeological ceramics. *Journal of Archaeological Science, 26*(3), 295–313. https://doi.org/10.1006/jasc.1998.0390

De Bonis, A., *et al.* (2018). Sr–Nd isotopic fingerprinting for ceramic provenance. *Journal of Archaeological Science, 94*, 98–108. https://doi.org/10.1016/j.jas.2018.04.005

Egozcue, J. J., *et al.* (2003). Isometric logratio transformations. *Mathematical Geology, 35*(3), 279–300. https://doi.org/10.1023/A:1023818214614

Folk, R. L. (1980). *Petrology of sedimentary rocks*. Hemphill Publishing.

Gal, M. (1974). Clay mineral distribution in Israeli soil types. *Journal of Soil Science, 25*(1), 79–86. https://doi.org/10.1111/j.1365–2389.1974.tb01105.x

Garfinkel, Y. (1993). The Yarmukian culture in Israel. *Paléorient, 19*(1), 115–134. https://doi.org/10.3406/paleo.1993.4589

Garfinkel, Y. (2019). *Shaar Hagolan Vol. 5: Early pyrotechnology*. Hebrew University.

Goren, Y. (2000). Petrographic characteristics of Southern Levantine ceramic materials. *Internet Archaeology, 9*. https://doi.org/10.11141/ia.9.5

Goren, Y., Finkelstein, I., & Na'aman, N. (2004). *Inscribed in clay*. Tel Aviv University.

Halicz, L., *et al.* (2008). Strontium stable isotopes in soil environments. *Earth and Planetary Science Letters, 272*, 406–411. https://doi.org/10.1016/j.epsl.2008.05.005

Hein, A., & Kilikoglou, V. (2020). Ceramic raw materials: Chemistry. *Archaeological and Anthropological Sciences, 12*, 180. https://doi.org/10.1007/s12520–020–01129–8

Kibaroğlu, M., & Falb, C. (2013). Southeast Anatolia Project archaeometric investigations. *Applied Clay Science, 82*, 53–61. https://doi.org/10.1016/j.clay.2013.06.016

Kibaroğlu, M., *et al.* (2017). Strontium isotope analysis of North–Mesopotamian metallic ware. *Journal of Archaeological Science: Reports, 16*, 370–382. https://doi.org/10.1016/j.jasrep.2017.08.027

Moffat, I., *et al.* (2020). Bioavailable strontium isotope data from Israel. *Earth System Science Data, 12*, 3641–3652. https://doi.org/10.5194/essd–12–3641–2020

Montana, G. (2020). Ceramic raw materials: Mineralogy, petrography. *Archaeological and Anthropological Sciences, 12*, 175. https://doi.org/10.1007/s12520–020–01130–1

Nesbitt, H. W., & Young, G. M. (1982). Early Proterozoic climates from lutite chemistry. *Nature, 299*, 715–717. https://doi.org/10.1038/299715a0

Quinn, P. S. (2013). *Ceramic petrography*. Archaeopress.

Rice, P. M. (2015). *Pottery analysis: A sourcebook* (2nd ed.). University of Chicago Press.

Roux, V., & Harivel, A. (2025). *Pottery chaîne opératoire at Shaar HaGolan*. CNRS.

Sandler, A. (2013). Clay distribution over the landscape of Israel. *Catena, 110*, 119–132. https://doi.org/10.1016/j.catena.2013.06.006

Sandler, A., *et al.* (2015). Mineralogical variability of mountain Mediterranean soils. *Geoderma, 235–236*, 398–413. https://doi.org/10.1016/j.geoderma.2014.07.032

Singer, A. (2007). *The soils of Israel*. Springer. https://doi.org/10.1007/978–3–540–71734–8

Singer, A., & Schwertmann, U. (1998). Iron oxide mineralogy of Terra Rossa and Rendzinas. *European Journal of Soil Science, 49*(3), 385–395. https://doi.org/10.1046/j.1365–2389.1998.4930385.x

Su, N., *et al.* (2017). REE fractionation during weathering and transport. *Geochemistry, Geophysics, Geosystems, 18*, 935–955. https://doi.org/10.1002/2016GC006659

Tite, M. S. (2008). Ceramic production, provenance and use. *Archaeometry, 50*(2), 216–231. https://doi.org/10.1111/j.1475–4754.2008.00391.x

Weigand, P. C., *et al.* (1977). Turquoise sources and source analysis. In T. K. Earle & J. E. Ericson (Eds.), *Exchange systems in prehistory* (pp. 15–34). Academic Press.

Yaalon, D. H. (1997). Soils in the Mediterranean region. *Catena, 28*, 157–169. https://doi.org/10.1016/S0341–8162(96)00035–5

Yaalon, D. H., & Ganor, E. (1973). The influence of dust on soils during the Quaternary. *Soil Science, 116*(3), 146–155. https://doi.org/10.1097/00010694–197309000–00003